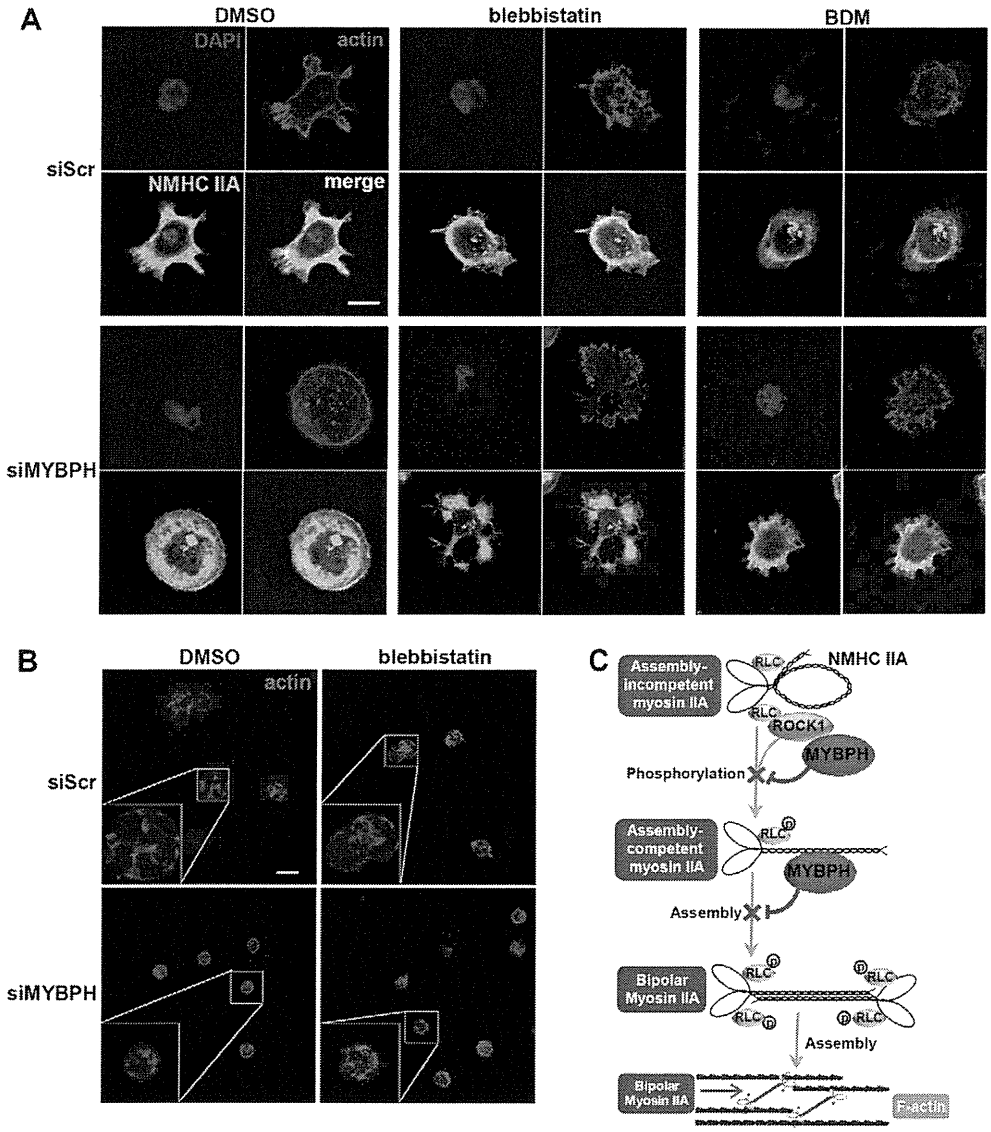

Fig. 4. siMYBPH-induced peripheral actomyosin bundle formation is counteracted by simultaneous treatment with non-muscle myosin inhibitors. (A) Immunofluorescence staining for actin (red) and NMHC IIA (green) in blebbistatin- or BDM-treated NCI-H441 cells. Immunofluorescence staining was performed as previously described [26]. Bar indicates 10 μm. (B) Three-dimensional Matrigel invasion assay in NCI-H441 cell treated with siMYBPH and/or blebbistatin. Three-dimensional Matrigel invasion assays were performed as previously described [26]. White bar indicates 50 μm. (C) Schematic diagram of multifaceted inhibitory roles of MYBPH in actomyosin organization at 2 distinct steps.

to search for MYBPH alterations in cases with similar disease phenotypes without NMHC IIA mutations.

In summary, our results demonstrate that MYBPH inhibits the assembly of NMHC IIA through direct binding to assembly-competent NMHC IIA, suggesting that this activity may in turn contribute to suppression of cancer invasion and metastasis together with its ROCK1 inhibitory function [26]. The dual roles of MYBPH in NM IIA inhibition comprise an intriguing mechanism to impose firm NM IIA inhibition. The present findings also provide clues for better understanding of the molecular mechanisms involved in inhibition of cancer invasion and metastasis by TTF-1 through transcriptional activation of MYBPH, as well as for better prognosis for TTF-1-positive lung adenocarcinoma patients.

Acknowledgments

This work was supported in part by Grants-in-Aid for Scientific Research on Innovative Areas from The Ministry of Education, Culture, Sports, Science and Technology (MEXT) of Japan, as well as a Grant-in-Aid for Young Scientists (B) from the Japan Society for the Promotion of Science (JSPS). Y.H. was supported by a research fellowship of the Foundation for Promotion of Cancer Research.

Appendix A. Supplementary data

Supplementary data associated with this article can be found, in the online version, at http://dx.doi.org/10.1016/j.bbrc.2012.10.036.

References

[1] D.A. Lauffenburger, A.F. Horwitz, Cell migration: a physically integrated molecular process, Cell 84 (1996) 359–369.

[2] P. Friedl, K. Wolf, Tumour-cell invasion and migration: diversity and escape mechanisms, Nat. Rev. Cancer 3 (2003) 362–374.

[3] A. Hall, The cytoskeleton and cancer, Cancer Metastasis Rev. 28 (2009) 5–14.

[4] M.A. Conti, R.S. Adelstein, Nonmuscle myosin II moves in new directions, J. Cell Sci. 121 (2008) 11–18.

[5] M. Vicente-Manzanares, X. Ma, R.S. Adelstein, A.R. Horwitz, Non-muscle myosin II takes centre stage in cell adhesion and migration, Nat. Rev. Mol. Cell Biol. 10 (2009) 778–790.
[6] V. Betapudi, L.S. Licate, T.T. Egelhoff, Distinct roles of nonmuscle myosin II isoforms in the regulation of MDA-MB-231 breast cancer cell spreading and migration, Cancer Res. 66 (2006) 4725–4733.
[7] Y. Huang, P. Arora, C.A. McCulloch, W.F. Vogel, The collagen receptor DDR1 regulates cell spreading and motility by associating with myosin IIA, J. Cell Sci. 122 (2009) 1637–1646.
[8] S. Medjkane, C. Perez-Sanchez, C. Gaggioli, E. Sahai, R. Treisman, Myocardin-related transcription factors and SRF are required for cytoskeletal dynamics and experimental metastasis, Nat. Cell. Biol. 11 (2009) 257–268.
[9] S. Etienne-Manneville, A. Hall, Rho GTPases in cell biology, Nature 420 (2002) 629–635.
[10] K. Riento, A.J. Ridley, Rocks: multifunctional kinases in cell behaviour, Nat. Rev. Mol. Cell Biol. 4 (2003) 446–456.
[11] K. Itoh, K. Yoshioka, H. Akedo, M. Uehata, T. Ishizaki, S. Narumiya, An essential part for Rho-associated kinase in the transcellular invasion of tumor cells, Nat. Med. 5 (1999) 221–225.
[12] E. Sahai, C.J. Marshall, ROCK and Dia have opposing effects on adherens junctions downstream of Rho, Nat. Cell Biol. 4 (2002) 408–415.
[13] S. Wilkinson, H.F. Paterson, C.J. Marshall, Cdc42-MRCK and Rho-ROCK signalling cooperate in myosin phosphorylation and cell invasion, Nat. Cell Biol. 7 (2005) 255–261.
[14] C.C. Wong, C.M. Wong, F.C. Ko, L.K. Chan, Y.P. Ching, J.W. Yam, I.O. Ng, Deleted in liver cancer 1 (DLC1) negatively regulates Rho/ROCK/MLC pathway in hepatocellular carcinoma, PLoS One 3 (2008) e2779.
[15] N.G. Dulyaninova, V.N. Malashkevich, S.C. Almo, A.R. Bresnick, Regulation of myosin-IIA assembly and Mts1 binding by heavy chain phosphorylation, Biochemistry 44 (2005) 6867–6876.
[16] Z.H. Li, A.R. Bresnick, The S100A4 metastasis factor regulates cellular motility via a direct interaction with myosin-IIA, Cancer Res. 66 (2006) 5173–5180.
[17] S. Kimura, Y. Hara, T. Pineau, P. Fernandez-Salguero, C.H. Fox, J.M. Ward, F.J. Gonzalez, The T/ebp null mouse: thyroid-specific enhancer-binding protein is essential for the organogenesis of the thyroid, lung, ventral forebrain, and pituitary, Genes Dev. 10 (1996) 60–69.
[18] Y. Yatabe, T. Mitsudomi, T. Takahashi, TTF-1 expression in pulmonary adenocarcinomas, Am. J. Surg. Pathol. 26 (2002) 767–773.
[19] T. Takeuchi, S. Tomida, Y. Yatabe, T. Kosaka, H. Osada, K. Yanagisawa, T. Mitsudomi, T. Takahashi, Expression profile-defined classification of lung adenocarcinoma shows close relationship with underlying major genetic changes and clinicopathologic behaviors, J. Clin. Oncol. 24 (2006) 1679–1688.
[20] H. Tanaka, K. Yanagisawa, K. Shinjo, A. Taguchi, K. Maeno, S. Tomida, Y. Shimada, H. Osada, T. Kosaka, H. Matsubara, T. Mitsudomi, Y. Sekido, M. Tanimoto, Y. Yatabe, T. Takahashi, Lineage-specific dependency of lung adenocarcinomas on the lung development regulator TTF-1, Cancer Res. 67 (2007) 6007–6011.
[21] J. Kendall, Q. Liu, A. Bakleh, A. Krasnitz, K.C. Nguyen, B. Lakshmi, W.L. Gerald, S. Powers, D. Mu, Oncogenic cooperation and coamplification of developmental transcription factor genes in lung cancer, Proc. Natl. Acad. Sci. USA 104 (2007) 16663–16668.
[22] B.A. Weir, M.S. Woo, G. Getz, S. Perner, L. Ding, R. Beroukhim, W.M. Lin, M.A. Province, A. Kraja, L.A. Johnson, K. Shah, M. Sato, R.K. Thomas, J.A. Barletta, I.B. Borecki, S. Broderick, A.C. Chang, D.Y. Chiang, L.R. Chirieac, J. Cho, Y. Fujii, A.F. Gazdar, T. Giordano, H. Greulich, M. Hanna, B.E. Johnson, M.G. Kris, A. Lash, L. Lin, N. Lindeman, E.R. Mardis, J.D. McPherson, J.D. Minna, M.B. Morgan, M. Nadel, M.B. Orringer, J.R. Osborne, B. Ozenberger, A.H. Ramos, J. Robinson, J.A. Roth, V. Rusch, H. Sasaki, F. Shepherd, C. Sougnez, M.R. Spitz, M.S. Tsao, D. Twomey, R.G. Verhaak, G.M. Weinstock, D.A. Wheeler, W. Winckler, A. Yoshizawa, S. Yu, M.F. Zakowski, Q. Zhang, D.G. Beer, Wistuba II, M.A. Watson, L.A. Garraway, M. Ladanyi, W.D. Travis, W. Pao, M.A. Rubin, S.B. Gabriel, R.A. Gibbs, H.E. Varmus, R.K. Wilson, E.S. Lander, M. Meyerson, Characterizing the cancer genome in lung adenocarcinoma, Nature 450 (2007) 893–898.
[23] K.A. Kwei, Y.H. Kim, L. Girard, J. Kao, M. Pacyna-Gengelbach, K. Salari, J. Lee, Y.L. Choi, M. Sato, P. Wang, T. Hernandez-Boussard, A.F. Gazdar, I. Petersen, J.D. Minna, J.R. Pollack, Genomic profiling identifies TITF1 as a lineage-specific oncogene amplified in lung cancer, Oncogene 27 (2008) 3635–3640.
[24] T. Yamaguchi, K. Yanagisawa, R. Sugiyama, Y. Hosono, Y. Shimada, C. Arima, S. Kato, S. Tomida, M. Suzuki, H. Osada, T. Takahashi, NKX2-1/TITF1/TTF-1-Induced ROR1 is required to sustain EGFR survival signaling in lung adenocarcinoma, Cancer Cell 21 (2012) 348–361.
[25] V.K. Anagnostou, K.N. Syrigos, G. Bepler, R.J. Homer, D.L. Rimm, Thyroid transcription factor 1 is an independent prognostic factor for patients with stage I lung adenocarcinoma, J. Clin. Oncol. 27 (2009) 271–278.
[26] Y. Hosono, T. Yamaguchi, E. Mizutani, K. Yanagisawa, C. Arima, S. Tomida, Y. Shimada, M. Hiraoka, S. Kato, K. Yokoi, M. Suzuki, T. Takahashi, MYBPH, a transcriptional target of TTF-1, inhibits ROCK1, and reduces cell motility and metastasis, EMBO J. 31 (2012) 481–493.
[27] A.F. Straight, A. Cheung, J. Limouze, I. Chen, N.J. Westwood, J.R. Sellers, T.J. Mitchison, Dissecting temporal and spatial control of cytokinesis with a myosin II inhibitor, Science 299 (2003) 1743–1747.
[28] L.P. Cramer, T.J. Mitchison, Myosin is involved in postmitotic cell spreading, J. Cell Biol. 131 (1995) 179–189.
[29] E. Flashman, C. Redwood, J. Moolman-Smook, H. Watkins, Cardiac myosin binding protein C: its role in physiology and disease, Circ. Res. 94 (2004) 1279–1289.
[30] C. Gaggioli, S. Hooper, C. Hidalgo-Carcedo, R. Grosse, J.F. Marshall, K. Harrington, E. Sahai, Fibroblast-led collective invasion of carcinoma cells with differing roles for RhoGTPases in leading and following cells, Nat. Cell Biol. 9 (2007) 1392–1400.
[31] C. Hidalgo-Carcedo, S. Hooper, S.I. Chaudhry, P. Williamson, K. Harrington, B. Leitinger, E. Sahai, Collective cell migration requires suppression of actomyosin at cell–cell contacts mediated by DDR1 and the cell polarity regulators Par3 and Par6, Nat. Cell Biol. 13 (2011) 49–58.
[32] K.M. Trybus, S. Lowey, Conformational states of smooth muscle myosin. Effects of light chain phosphorylation and ionic strength, J. Biol. Chem. 259 (1984) 8564–8571.
[33] E.J. Kim, D.M. Helfman, Characterization of the metastasis-associated protein, S100A4. Roles of calcium binding and dimerization in cellular localization and interaction with myosin, J. Biol. Chem. 278 (2003) 30063–30073.
[34] J.D. Franke, F. Dong, W.L. Rickoll, M.J. Kelley, D.P. Kiehart, Rod mutations associated with MYH9-related disorders disrupt nonmuscle myosin-IIA assembly, Blood 105 (2005) 161–169.
[35] Y. Zhang, M.A. Conti, D. Malide, F. Dong, A. Wang, Y.A. Shmist, C. Liu, P. Zerfas, M.P. Daniels, C.C. Chan, E. Kozin, B. Kachar, M.J. Kelley, J.B. Kopp, R.S. Adelstein, Mouse models of MYH9-related disease: mutations in nonmuscle myosin II-A, Blood 119 (2012) 238–250.

Hindawi Publishing Corporation
International Journal of Proteomics
Volume 2012, Article ID 510397, 11 pages
doi:10.1155/2012/510397

Research Article

Seven-Signal Proteomic Signature for Detection of Operable Pancreatic Ductal Adenocarcinoma and Their Discrimination from Autoimmune Pancreatitis

Kiyoshi Yanagisawa,[1,2] Shuta Tomida,[2] Keitaro Matsuo,[3] Chinatsu Arima,[2] Miyoko Kusumegi,[4] Yukihiro Yokoyama,[5] Shigeru B. H. Ko,[6] Nobumasa Mizuno,[7] Takeo Kawahara,[5] Yoko Kuroyanagi,[8] Toshiyuki Takeuchi,[8] Hidemi Goto,[6] Kenji Yamao,[7] Masato Nagino,[5] Kazuo Tajima,[3] and Takashi Takahashi[2]

[1] *Institute for Advanced Research, Nagoya University, Furo-cho, Chikusa-ku, Nagoya 464-8601, Japan*
[2] *Division of Molecular Carcinogenesis, Center for Neurological Diseases and Cancer, Nagoya University Graduate School of Medicine, Nagoya 466-8550, Japan*
[3] *Division of Epidemiology and Prevention, Aichi Cancer Center, Nagoya 464-8681, Japan*
[4] *Division of Research and Development, Oncomics Co., Ltd., Nagoya 464-0858, Japan*
[5] *Division of Surgical Oncology, Department of Surgery, Nagoya University Hospital, Nagoya 466-8550, Japan*
[6] *Department of Gastroenterology, Nagoya University Hospital, Nagoya 466-8550, Japan*
[7] *Department of Gastroenterology, Aichi Cancer Center, Nagoya 464-8681, Japan*
[8] *Division of Research and Development, Oncomics Co., Ltd, Nagoya 464-0858, Japan*

Correspondence should be addressed to Kiyoshi Yanagisawa, kyana@med.nagoya-u.ac.jp

Received 27 January 2012; Accepted 9 March 2012

Academic Editor: Visith Thongboonkerd

There is urgent need for biomarkers that provide early detection of pancreatic ductal adenocarcinoma (PDAC) as well as discrimination of autoimmune pancreatitis, as current clinical approaches are not suitably accurate for precise diagnosis. We used mass spectrometry to analyze protein profiles of more than 300 plasma specimens obtained from PDAC, noncancerous pancreatic diseases including autoimmune pancreatitis patients and healthy subjects. We obtained 1063 proteomic signals from 160 plasma samples in the training cohort. A proteomic signature consisting of 7 mass spectrometry signals was used for construction of a proteomic model for detection of PDAC patients. Using the test cohort, we confirmed that this proteomic model had discrimination power equal to that observed with the training cohort. The overall sensitivity and specificity for detection of cancer patients were 82.6% and 90.9%, respectively. Notably, 62.5% of the stage I and II cases were detected by our proteomic model. We also found that 100% of autoimmune pancreatitis patients were correctly assigned as noncancerous individuals. In the present paper, we developed a proteomic model that was shown able to detect early-stage PDAC patients. In addition, our model appeared capable of discriminating patients with autoimmune pancreatitis from those with PDAC.

1. Introduction

Pancreatic ductal adenocarcinoma (PDAC) is the fifth leading cause of cancer death in Japan with more than 24,000 deaths annually [1], while 35,000 deaths each year in the United States are caused by the disease [2]. Long-term survival for PDAC patients remains unsatisfactory, with only 3–5% surviving for more than 5 years after surgical resection, with the remainder succumbing to widespread metastasis or massive local recurrence. Since surgical resection is the only reliable curative treatment, early detection is essential to improve the outcomes of affected individuals. However, the clinical symptoms of PDAC are often unremarkable until advanced stages of the disease, and the anatomic

location of the pancreas deep in the abdomen makes physical detection and imaging approaches difficult. Thus, less than 10% of patients diagnosed with PDAC are eligible for surgical resection [3]. Although serum markers for PDAC including carcinoembryonic antigen (CEA) and carbohydrate antigen 19-9 (CA19-9) play important roles in current clinical practice for monitoring progression and treatment response, as well as surveillance for recurrence, these markers are not ideal for cancer screening due to their low specificity and/or sensitivity in early stages of the disease [4–6].

The concept of autoimmune pancreatitis (AIP) is supported by recent advances in elucidating its pathogenesis as a unique systemic disease. AIP has several characteristic features, such as infiltration of CD4-positive T cells and IgG4-positive plasmacytes, irregular narrowing of the pancreatic duct, and diffuse enlargement of the pancreas [7–9]. Although intensive investigations into the pathogenesis of AIP have been conducted, its underlying molecular mechanism remains unclear. The most important and difficult step in diagnosing AIP is to distinguish it from PDAC. Clinical symptoms such as obstructive jaundice are not helpful for discrimination, while IgG4, the most accurate serum marker for AIP, is not adequately specific to exclude the existence of cancer. Furthermore, AIP is sometimes accompanied by PDAC; thus percutaneous or endoscopic biopsy findings are often needed for final diagnosis. Unfortunately, those examinations are invasive for the patient and may fail to detect small regions of cancer cells. As a result, unnecessary surgery because of misdiagnosis performed for AIP patients without cancer or those undergoing treatment for existing cancer is a critical issue in clinical practice. Accordingly, there is urgent need for elucidation of novel biomarker(s) and noninvasive diagnostic strategies useful for early detection of PDAC, as well as discrimination of patients with AIP to improve clinical management and prognosis.

Comprehensive analysis of protein expression patterns in biological materials might improve understanding of the molecular complexities of human diseases [10] and could be useful to detect diagnostic or predictive protein expression patterns that reflect clinical features. Matrix-assisted laser desorption/ionization mass spectrometry (MALDI MS) can profile proteins up to 50 kDa in size in serum, tissues, and other various clinical specimens. Protein profiles obtained may contain thousands of data points and provide proteomic signatures that allow detection of patients with various diseases [11, 12]. We previously employed MALDI MS for expression profiling of proteins in human lung cancer specimens and found that the resultant proteomic patterns could predict various clinical features, as well as the potential of recurrence in stage I lung cancer patients [13, 14].

In the present study, protein expression profiling with MALDI MS was conducted to identify proteomic patterns in plasma samples for discrimination of PDAC from AIP as well as chronic pancreatitis (CP) using 3 independent datasets. We found that a proteomic model consisting of 7 mass spectrometry signals constructed by use of the training cohort could detect 82.6% (38 of 46, 95% CI 68.6–92.2) of known PDAC cases, including 62.5% (5 of 8, 95% CI 24.5–91.5) of the stage I and II cases in the independent test cohort, which successfully confirmed its discrimination power. We further applied our model for discrimination of AIP as well as CP from PDAC and found that it correctly assigned 100% of the AIP and CP patients (19 of 19, 95% CI 82.4–100 and 11 of 11, 95% CI 71.5–100, resp.) as noncancerous. These results indicate that our 7-signal proteomic model may contribute to accurate decisions regarding the therapeutic plan for patients with chronic pancreatic diseases, especially PDAC and AIP.

2. Methods

2.1. Patients and Specimens. Plasma specimens from 96 PDAC patients were obtained from the Department of Epidemiology and Prevention, Aichi Cancer Center Research Institute, Nagoya, Japan, collected from January 2001 and November 2005. Of those, 80 were randomly assigned to the training set and 16 to the test set. An additional 30 plasma specimens from PDAC patients were obtained from the Department of Surgery, Nagoya University Hospital, Nagoya, Japan, collected from May 2004 to July 2006, and assigned to the test set. Plasma specimens from 147 healthy control subjects were also obtained from the Department of Epidemiology and Prevention, Aichi Cancer Center Research Institute, and used. Of those, 80 were randomly assigned to the training set and 67 to the test set. Plasma specimens from 2 acute pancreatitis, 11 chronic pancreatitis, and 3 autoimmune pancreatitis patients were obtained from the Department of Gastroenterology, Nagoya University Hospital, collected from April 2005 and November 2007, and assigned to the test set. In addition, 16 plasma specimens from autoimmune pancreatitis were obtained from the Department of Gastroenterology, Nagoya University Hospital, collected from September 2003 and August 2009, and assigned to the confirmation set. More detailed information is available in Supplementary Material available on line at doi: 10.1155/2012/510397. The characteristics of the patients and healthy subjects in the training, test, and confirmation cohorts are summarized in Supplementary Table S1, which shows that there were no statistically significant differences in regard to clinicopathologic features among the cohorts. All specimens were processed in the same manner and stored at −80°C within 180 minutes after being collected from the patients and healthy subjects, and not thawed until analysis. Requisite approval from our institutional review boards and written informed consent from all subjects were obtained. One plasma specimen per patient or healthy subject was analyzed, and the training, test, and confirmation datasets were independently analyzed as different batches. Further details are available in supplementary Material.

2.2. Proteomic Analysis. Five microliters of nonpre-treated plasma was mixed with 5 nL drops of an energy absorbing matrix solution (saturated Sinapinic acid in water/acetonitrile/trifluoroacetic acid (500 : 500 : 1, by volume), which allows molecules to be protonated and desorbed from tissue surfaces). Then, 1 μL mixtures were deposited into individual wells of MALDI MS sample plates (PE Biosystems, Foster

City, CA) and dried at room temperature for 5 minutes. Six spots were generated for each plasma-matrix mixture sample and spectra were acquired from all 6 using a 4800 Instrument (Applied Biosystems, Foster City, CA), essentially as described previously [13, 14]. Further details are available in Supplementary Material.

2.3. Statistical Methods. Protein profiles obtained by MALDI MS were analyzed using 3 distinct statistical methods, Fisher's exact test, the Kruskal-Wallis test, and a significance analysis of microarray (SAM) test [15], to investigate MS signals that appeared to differentiate PDAC patients from healthy individuals in the training set. MS signals that met at least 1 of the 3 selection criteria were further analyzed.

To construct a generally applicable proteomic classifier without specifically overfitting it to the training cohort, we used a weighted voting algorithm, a well-established technique for supervised classification, in which each weight value was calculated as the signal-to-noise ratio and a leave-one-out cross-validation strategy was utilized [16].

It is possible that unintended biased resubstitution or partial cross-validation can result in underestimation of the error rate after cross-validation; thus the performance of any class prediction rule is best assessed by applying the rule created by use of 1 dataset (the training set) to an independent dataset (the validation or test set) [17]. In the present study, the proteomic classifier constructed with the training dataset of 160 individuals was validated using a completely independent validation set composed of 145 individuals.

An agglomerative hierarchical clustering algorithm was applied to investigate the pattern among the statistically significant discriminator proteins as well as the biological status with Eisen's software [18].

2.4. Identification of Individual Proteins in the Proteomic Signature. 40 μ of serum samples was pretreated with high abundant protein depletion column (Agilent, Palo Alto, CA) according to manufacturer's instruction. The pretreated serum samples were separated over a polymeric column (Toso, Tokyo, Japan) with a high-performance liquid chromatography (HPLC) pump (Shimadzu, Osaka, Japan) and HPLC fractions were collected every minute for 80 minutes. Each fraction was lyophilized, reconstituted with a 50% acetonitrile in water containing 0.1% trifluoroacetic acid, and analyzed by MALDI mass spectrometry to identify the HPLC fractions that contained proteins corresponding to the peaks in the signature with molecular weights selected by bioinfomatic analysis as candidate molecular markers for the PDAC. The selected fractions were lyophilized and reconstituted with a mixture of 10 μL of 0.4 M ammonium hydrogen carbonate and 5 μL of 45 mM dithiothreitol, and then 10 μL of 100 mM iodoacetamide was added. This mixture was incubated for 4 hours at 37°C with 5 μL of 200 nM mass-grade trypsin (Promega, Madison, WI) to obtain peptides. The peptides were separated and sequenced by a microcapillary reverse-phase column (KYA technologies, Tokyo, Japan) with an HPLC pump (KYA) and MALDI mass spectrometer (Applied Biosystems). These spectra were compared with those in the human databases of the National Center for Biotechnology Information (nonredundant) by use of Mascot version 2.1.0 (Matrix Science Inc., Boston, MA). A minimum of two peptide matches and a positive association between the m/z values detected with MALDI mass spectrometry and the molecular weight of the intact protein (including posttranslational modifications) were required for protein identification.

3. Results

3.1. Protein Expression Profiling in the Training Cohort. We obtained protein expression profiles for the 160 human plasma specimens obtained from 80 PDAC patients and 80 healthy subjects at Aichi Cancer Center (Figure 1(a)) and Supplementary Table S1) using MALDI MS. Spectra were obtained from 6 replicates of single plasma specimens. MarkerView (Applied Biosystems) and custom software were used to bin the peaks across the spectra obtained from 960 samples, and then we calculate the average intensity of each signal individually among the 160 cases. As a result, we obtained expression profiles containing 1063 distinct proteomic signals. To extract a proteomic signature able to discriminate PDAC patients from healthy individuals, we compared MS signals from the 80 healthy subjects and 80 PDAC patients using our statistical selection criteria (signals met at least 2 of the following criteria: P value corrected with Bonferroni was less than 0.05 in Fisher's exact test and Kruskal-Wallis test, and FDR < 0.1% for SAM). As a result, 134 MS signals were found to be differentially expressed. Agglomerative hierarchical clustering analysis using the identified proteomic signature showed a clear separation of plasma specimens from PDAC patients as compared to those from healthy individuals (Figure 1(b)), which confirmed that the selected MS signals were informative for discrimination of PDAC cases from healthy individuals. The left branch mostly consisted of PDAC cases (81.3%, 65 of 80 cases, 95% CI 71.0–89.1), whereas the right branch consisted of healthy subjects (78.8%, 63 of 80 cases, 95% CI 68.2–87.1). Next, we investigated whether our proteomic prediction model could best distinguish noncancerous individuals from cancer patients. For this purpose, the 134 selected MS signals, which were informative for discrimination, were further ranked according to the SAM and weighted-voting proteomic discriminatory models were constructed using increasing numbers of the differentially expressed proteomic signals (up to 134), for which learning errors were calculated by leave-one-out cross-validation (Figure 2(a)). This cross-validation analysis showed that the use of 7 MS signals gave the lowest number of misclassifications, while 7 MS signals (8562.3, 8684.4, 8765.1, 9423.5, 13761.5, 14145.2, and 17250.8 m/z) were extracted as the most shared ones. Using this proteomic model, plasma samples from both PDAC patients and healthy subjects were classified as either positive or negative for cancer, which showed that the sensitivity for prediction was 76.3% (61 of 80 of the cancer patients, 95% CI 65.4–85.1) and for specificity was 91.3% (73 of 80 of the healthy subjects, 95% CI 82.8–96.4, Table 1), for an overall

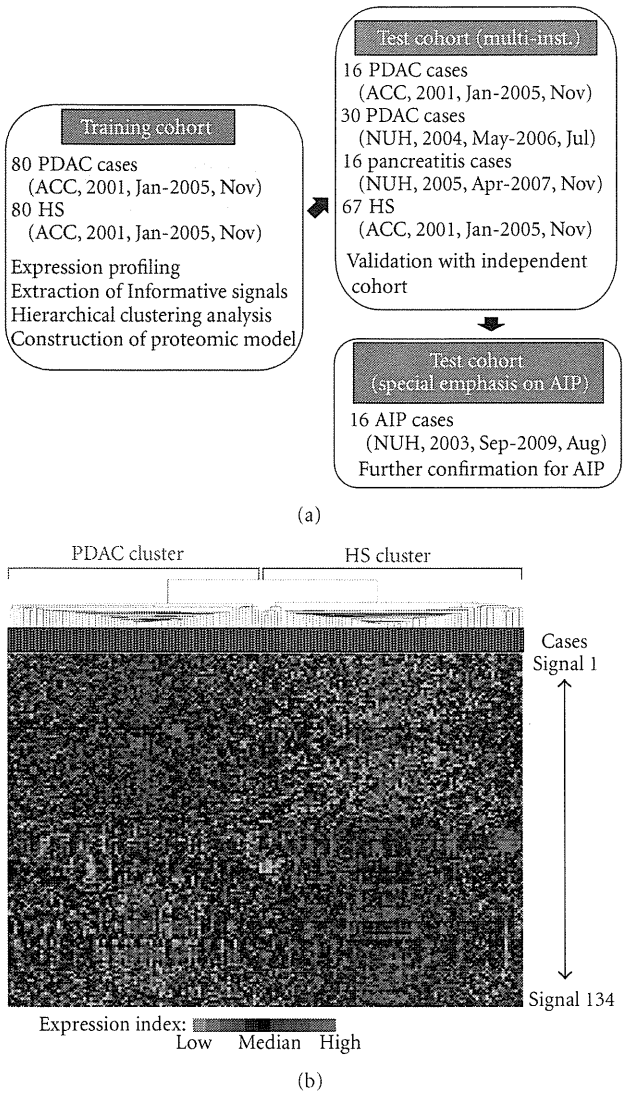

FIGURE 1: MALDI MS analysis of plasma specimens from human PDAC patients and healthy subjects in the training cohort. (a) Independent training-validation-confirmation datasets of 160 training cases, 129 validation cases, and 16 confirmation cases. (b) Unsupervised hierarchical clustering analysis of 80 human PDAC patients and 80 healthy subjects in the training cohort according to the protein expression patterns of 134 MS signals. Each row represents an individual proteomic signal and each column an individual sample. The dendrogram at the top shows the similarities in protein expression profiles among the samples. Substantially elevated (red) expression of the proteins was observed in individual plasma samples. HS: healthy subjects; PDAC: pancreatic ductal adenocarcinoma. Red box case: PDAC: blue box case: healthy subject.

classification accuracy of 83.8% (134 of 160, 95% CI 77.1–89.1). We also calculated positive and negative predictive values (PPV and NPV, resp.) to confirm the diagnostic power of our model, which were 89.8% and 79.3%, respectively. We observed no significant difference for detection of PDAC patients related to lymph node positivity and prognosis. Furthermore, we analyzed the relationship between the age of PDAC patients (≤60 or >60 years old) and detection power of the 7 MS signals. Those results showed that the sensitivity for prediction was 69.8% (30 of 43, 95% CI 53.9–82.8) and 83.8% (31 of 37, 95% CI 68.0–93.8) in the younger and older groups, respectively (Table 1), with no significance in discrimination found ($P = 0.142$, Fisher's exact test). Representative spectra that comprised the 7-signal proteomic model for the healthy subjects and PDAC patients are shown in Figure 2(b). It is of note that our model was able to correctly distinguish 72.7% (8 of 11 cases, 95% CI 39.0–94.0) of the stage I and II cases from the healthy subjects, while it also correctly classified 78.8% (26 of 33, 95% CI 61.1–91.0) of the PDAC patients eligible for surgical resection as positive for cancer (Table 1).

3.2. Protein Expression Profiling in the Test Cohort. It has been well reported that the robustness, including accuracy, of a prediction model should be assessed using an independent validation cohort, even when cross-validation methods, such as LOOCV or n-fold CV, were properly used for developing the prediction model [19]. To examine the robustness of the 7-signal proteomic model constructed with data from MALDI-MS analysis of the training cohort, we applied it to an independent test dataset obtained from plasma samples collected at two different institutions. We also determined whether the identified proteomic model could discriminate between acute and chronic pancreatitis patients, as well as autoimmune pancreatitis, as the discovery of biomarkers applicable for differential diagnosis between PDAC and noncancerous pancreatic diseases has great potential for clinical practice. For the test cohort, plasma samples were obtained from 46 PDAC patients (16 and 30 cases of ACC and NUH, resp.) and 67 healthy subjects from the ACC group, while 16 pancreatitis samples obtained from Nagoya University hospital (NUH) consisted of 2 acute pancreatitis, 11 chronic pancreatitis, and 3 autoimmune pancreatitis cases (Figure 1(a), Supplementary Tables S1 and S2 for additional clinical information for AIP patients). With the 7-signal proteomic model, 82.6% (38 of 46, 95% CI 68.6–92.2) of the cancer cases were classified into the positive group, while 89.2% (74 of 83, 95% CI 80.4–94.9) of the noncancerous subjects were assigned to the group negative for cancer (Figure 3 and Table 2). We calculated PPV and NPV, which were 80.9% and 90.2%, respectively, and the overall accuracy of the classification with the test cohort was 86.8% (112 of 129, 95% CI 79.7–92.1). We also evaluated the relationship between blood vessel invasion (surgery with or without mesenteric venous tract resection) and detection power of the 7 MS signals. Our results showed that the sensitivity for prediction was 88.8% (8 of 9, 95% CI 51.8–99.7) for PDAC patients who underwent mesenteric venous tract resection and 78.6% (11 of 14, 95% CI 49.2–95.3) for those who did not, with no significant difference found ($P = 0.524$, Fisher's exact test). Future studies with a larger number of PDAC patients treated with surgery are warranted to validate the clinical usefulness of our 7-signal proteomic signature. It is of note that our model was able to correctly distinguish 62.5%

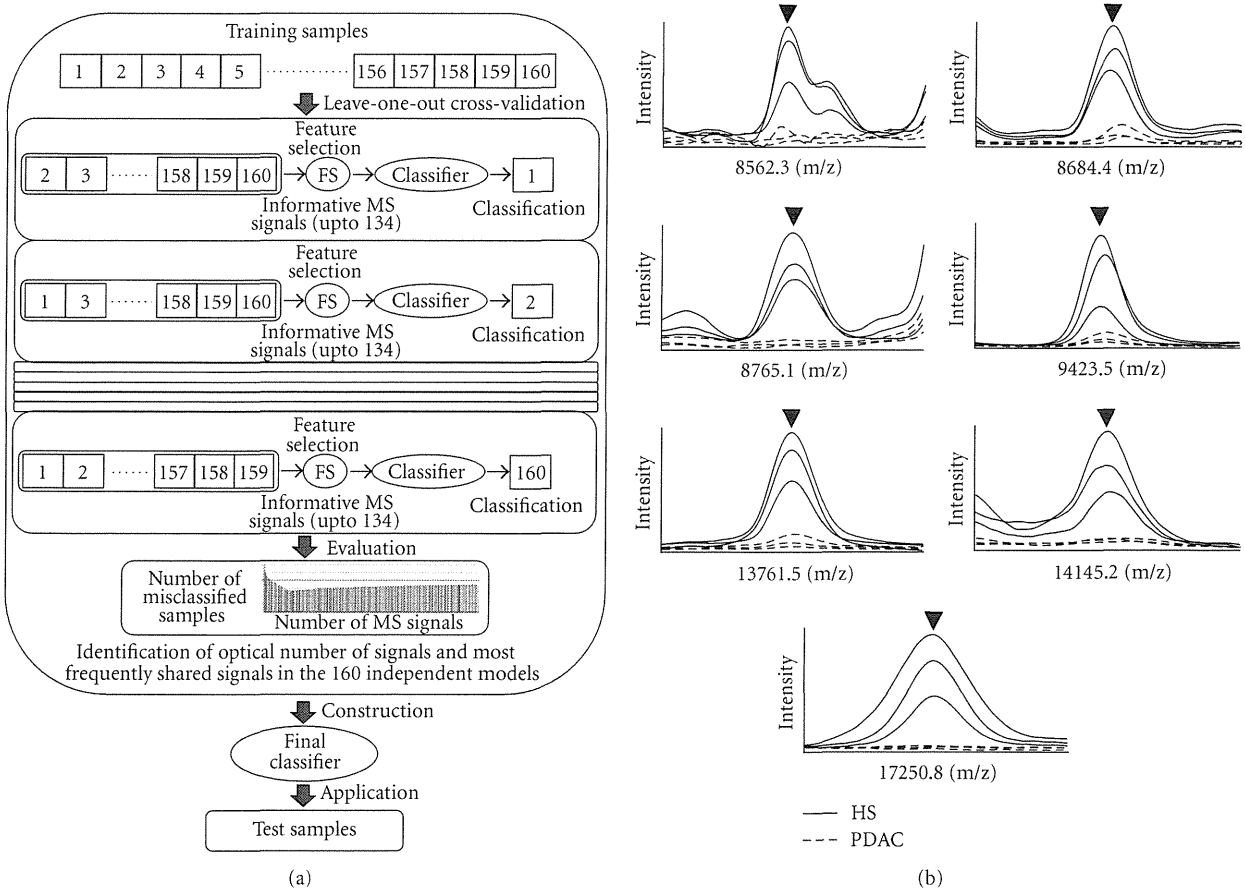

FIGURE 2: Construction of proteomic model for discrimination of PDAC cases from healthy subjects. (a) Schematic diagram of construction of proteomic discrimination model. (b) Representative mass spectra comprising 7-signal proteomic signature. Arrowheads show informative peaks for discrimination between healthy subjects and PDAC patients. Blue lines show representative spectra from healthy subjects and red lines show representative spectra from PDAC patients.

TABLE 1: Discrimination of samples in the training cohort according to 7-signal proteomic model.

	Number of cases analyzed	Number of correctly assigned cases (%)	95% C.I.* (%)
All samples	160	134 (83.8)	77.1–89.1
Pancreatic ductal adenocarcinoma	80	61 (76.3)	65.4–85.1
Healthy subjects	80	73 (91.3)	82.8–96.4
age			
≤60	43	30 (69.8)	53.9–82.8
>60	37	31 (83.8)	68.0–93.8
Clinical stage of pancreatic ductal adenocarcinoma patients			
0/I	3	3 (100)	29.2–100
II	8	5 (62.5)	24.5–91.5
III	8	8 (100)	63.1–100
IVa	14	10 (71.4)	41.9–91.6
IVb	47	35 (74.5)	59.7–86.1

* 95% confidence interval.

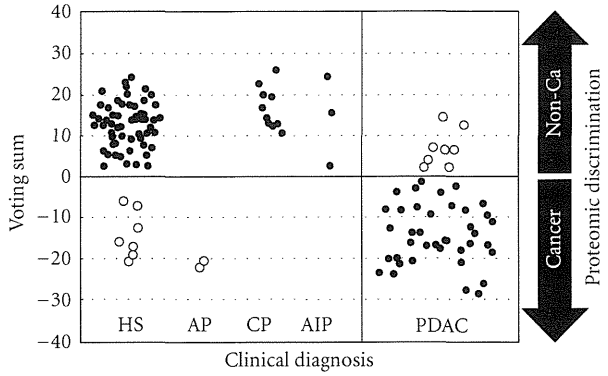

FIGURE 3: Assessment of 7-signal proteomic model with the validation cohort using weighted voting algorithm. The results of proteomic analyses of the training cohort are shown. Each circle represents a voting sum for a single patient. Solid circles: specimens whose prediction with proteomic model matched clinical diagnosis; open circles: specimens whose prediction with proteomic model did not match clinical diagnosis; HS: healthy subjects; AP: acute pancreatitis; CP: chronic pancreatitis; AIP: autoimmune pancreatitis; PDAC: pancreatic ductal adenocarcinoma.

(5 of 8 cases, 95% CI 24.5–91.5) of the stage I and II cases from the healthy subjects and also classified 78.9% (30 of 38, 95% CI 62.7–90.5) of the PDAC patients eligible for surgical resection as positive for cancer. It is also noteworthy that the identified proteomic model distinguished 100% of the patients with chronic pancreatitis (11 of 11, 95% CI 71.5–100) and AIP (3 of 3, 95% CI 29.2−100) from cancer cases (Figure 3 and Table 2).

3.3. Discrimination of Autoimmune Pancreatitis from PDAC Using 7-Signal Proteomic Model. Autoimmune pancreatitis is a systemic inflammatory disease of the pancreas and several diagnostic criteria have been proposed. However, their usefulness is under debate and accurate differential diagnosis remains difficult. Moreover, an important step in diagnosing AIP is to discriminate it from PDAC. In the present study, all (3 of 3) of the AIP patients were correctly discriminated from those with PDAC in the analysis with the test dataset; thus we next performed a confirmatory analysis using plasma samples collected from 16 AIP patients treated at NUH (Figure 1(a) and Supplementary Table S2). For this, we employed our 7-signal proteomic model to investigate whether it would classify the AIP patients as noncancerous and found that it correctly assigned those patients as negative for cancer with 100% accuracy (16 of 16 cases, 95% CI 79.4–100). Therefore, the high potential for discrimination of AIP from PDAC was validated with an independent confirmatory dataset used in a blinded manner. The serum level of CA19-9 was elevated in 4 (21.1%, 95% CI 7.3−52.4) of the AIP cases in our cohort, while IgG4 levels have been reported to be elevated in 10–30% of PDAC cases [7, 20]. Thus, our proteomic model may be applicable as a novel serological test to discriminate AIP from PDAC in clinical practice. Representative spectra obtained from the AIP and PDAC cases are shown in Figure 4.

3.4. Combination of MALDI Proteomic Signature and CA19-9 for Cancer Screening. Our 7-signal proteomic model was able to detect 82.6% (38 of 46, 95% CI 68.6–92.2) of the PDAC patients in the test cohort (Table 2). Moreover, it assigned 78.9% (30 of 38, 95% CI 62.7–90.5) of the patients eligible for an operation to the cancerous group, while 62.5% (5 of 8 and 95% CI 24.5–91.5) of the stage I and II cases were also detected with the identified model. Since it is possible that our 7-signal proteomic model and CA19-9 level are complementary, we investigated whether their combined use would improve the detection rate of patients who may benefit from surgery. The overall sensitivity of CA19-9 (cutoff value, 37 units/mL) alone for stage 0–IVa patients was 71.1% (27 of 38, 95% CI 54.1–84.6), while a combination of our 7-signal proteomic model and CA19-9 level detected 89.5% (34 of 38, 95% CI 75.2–97.1) of operable cases. Notably, for detection of stage I and II PDAC patients, CA19-9 assigned only 50.0% (4 of 8, 95% CI 15.7–84.3) of the cases to the positive group and no additional discrimination power of that marker was observed when combined with our proteomic model. Accordingly, we consider that our 7-signal proteomic model might be more sensitive for detection of early stage PDAC patients than CA19-9, which would improve clinical outcomes following surgical treatment.

3.5. Identification of Individual Proteins in the Proteomic Signature. As an initial step toward elucidating the biologic mechanism of the association between the proteomic signature and carcinogenesis, we identified a couple of proteins that correspond to the mass spectrometry signals in the proteomic signature obtained from serum. Extracts from two serum samples of healthy individual were fractionated by reverse phase-HPLC and analyzed by MALDI MS to identify the HPLC fractions that contained proteins corresponding to peaks in the proteomic signature. These selected fractions were subjected to sequence analysis of tryptic peptides by use of MALDI MS. Accordingly, we identified the following proteins as part of the proteomic signature: apolipoprotein A-I ($[M + H]^+$ = 17,250.8 m/z) and C-III ($[M + H]^+$ = 8765.1), and transthyretin ($[M + H]^+$ = 13761.5).

4. Discussion

In the present study, we analyzed the protein expression profiles of plasma specimens obtained from patients with PDAC, as well as acute and chronic pancreatitis cases, and autoimmune pancreatitis (AIP) patients with MALDI MS. Using bioinformatic analysis, we derived 7 MS signals that allowed us to produce a proteomic model for discrimination of PDAC from noncancerous individuals. When we used our proteomic model with both independent test cohort and confirmation group, 62.5% (5 of 8, 95% CI 24.5–91.5) of stage 0–II cases were correctly assigned to the cancerous group, while all AIP patients (19 of 19, 95% CI 82.4–100)

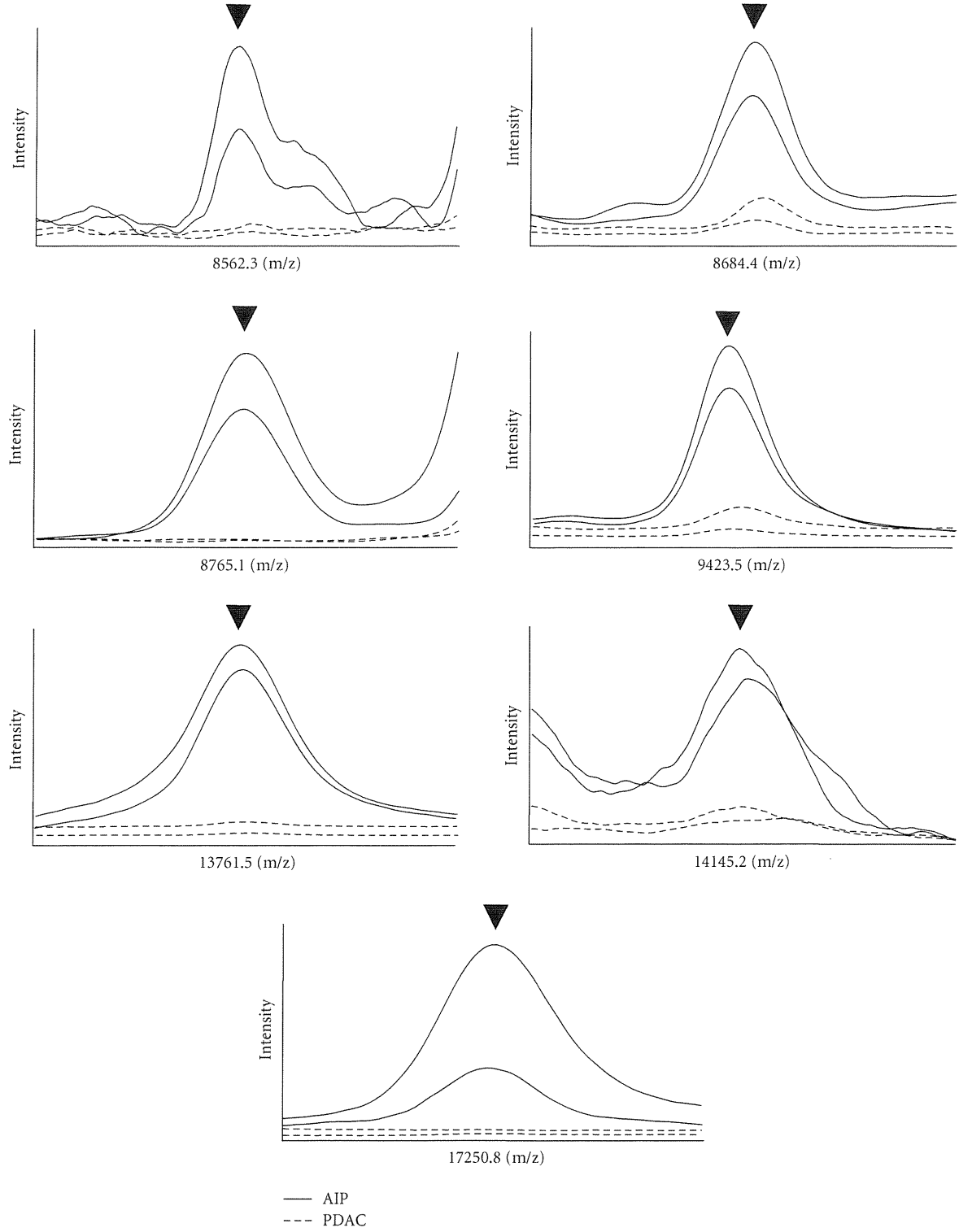

FIGURE 4: Representative mass spectra comprising 7-signal proteomic signature in autoimmune pancreatitis patients and PDAC patients. Arrowheads show informative peaks for discrimination between autoimmune pancreatitis patients and patients with pancreatic cancer. Blue solid and dotted lines show representative spectra from autoimmune pancreatitis patients, and red solid and dotted lines show representative spectra from pancreatic cancer patients. AIP: autoimmune pancreatitis; PDAC: pancreatic ductal adenocarcinoma.

Table 2: Discrimination of samples in the test cohort according to 7-signal proteomic model.

	Number of cases analyzed	Number of correctly assigned cases (%)	95% C.I.* (%)
All samples	129	112 (86.8)	79.7–92.1
Healthy subjects	67	60 (89.6)	79.7–95.7
Pancreatic ductal adenocarcinoma (ACCH)	16	13 (81.3)	54.4–96.0
Pancreatic ductal adenocarcinoma (NUH)	30	25 (83.3)	65.3–94.4
Acute pancreatitis (NUH)	2	0 (0)	0–84.2
Chronic pancreatitis (NUH)	11	11 (100)	71.5–100
Autoimmune pancreatitis (NUH)	3	3 (100)	29.2–100
Clinical stage of pancreatic ductal adenocarcinoma patients at ACCH			
0/I	0	NA	NA
II	1	0 (0)	0–97.5
III	3	3 (100)	29.2–100
IVa	4	2 (50)	6.8–93.2
IVb	8	8 (100)	63.1–100
Clinical stage of pancreatic ductal adenocarcinoma patients at NUH			
0/I	1	0 (0)	0–97.5
II	6	5 (83.3)	35.9–99.6
III	13	11 (84.6)	54.6–98.1
IVa	10	9 (90)	55.5–99.7
IVb	0	NA	NA

* 95% confidence interval
NA: not available.

were correctly assigned to the noncancerous group. Discrimination of AIP from cancer is obviously important; however it is currently problematic in clinical practice. Although previous reports have shown discrimination power of proteomic signature between PDAC patients and control subjects [21–24], to the best of our knowledge, the present 7-signal proteomic model is the first system of proteomic prediction based upon mass spectrometry found capable to both detect early-stage PDAC cases and discriminate AIP patients.

Early detection is essential for improving the outcomes of PDAC patients. However, those in stages 0–II are difficult to detect with current diagnostic approaches, including computerized tomography scanning, positron emission tomography scanning, and tissue-based diagnostic tests. CA19-9 is a tumor marker widely used for evaluations of therapeutic effects and detection of PDAC recurrence, though it is not considered to be applicable for mass screening when used alone [4, 6, 25, 26]. Recent advances in molecular biology have also revealed that clinical features cannot be adequately characterized or predicted by a single marker. Thus, microarray analysis has been employed to simultaneously investigate the expression levels of thousands of genes and identify mRNA patterns associated with various human diseases including PDAC [27–29]. However, mRNA expression does not always indicate which of the corresponding proteins are expressed or provide information regarding their post-translational regulation. Moreover, blood and body fluids, such as pancreatic juice and urine, do not contain mRNA. Thus, proteome analysis of such specimens is considered to better reflect the underlying clinical characteristics of human diseases as compared to gene expression profiling, while proteomic technologies including MS have been employed to analyze proteomes in clinical specimens [10–14, 30–32]. Previous proteomics studies of PDAC with healthy controls have shown promising results in distinguishing PDAC, with a sensitivity ranging from 78 to 91% and specificity from 75 to 100% [21–24, 33, 34]. These discrimination power results are better than those obtained with the current CA19-9 marker, while improved diagnostic performance has been observed when serum MS markers were combined with CA19-9 [21, 22, 24]. In the present study, we found that the combination of our 7-signal proteomic model and CA19-9 level improved the positive rate of detection of PDAC patients eligible for surgical resection to 89.5% (34 of 38, 95% CI 75.2–97.1). It is noteworthy that detection of stage I-II cases was also attainable at a sensitivity of 62.5% (5 of 8, 95% CI 24.591.5) without further improvement by adding CA19-9. These results support the usefulness of our 7-signal proteomic model for detection of early stage cases. Since we constructed the present 7-signal model independent from CA19-9, further optimization of selection of a proteomic signature with focus on early detection possibly along with adjustment of the CA19-9 cutoff value is warranted to obtain increased sensitivity. The present 7-signal proteomic model showed high potential to assign inflammatory pancreatic disease patients to the noncancerous group (93.8%; 30 of 32, 95% CI 79.2–99.2). Interestingly, 2 of the misclassified

patients suffered from acute pancreatitis; however, all of the patients of chronic pancreatitis and AIP (11 of 11, 95% CI 71.5–100; and 19 of 19, 95% CI 82.4–100) were correctly assigned to the noncancerous group by our proteomic model. Discrimination of AIP from PDAC is difficult in clinical practice, as symptoms such as obstructive jaundice or space occupying lesions in the pancreas are commonly observed in both cases. Actually, most of the AIP patients in this study showed at least one of these symptoms. Our proteomic model distinguished between AIP patients and those with PDAC with high accuracy; thus it is considered to be effective in future clinical applications, especially for selecting those who are eligible for invasive diagnostic procedures followed by inevitably invasive surgical treatment for PDAC. During the course of our study, Frulloni et al. reported that autoantigens against the plasminogen binding protein of helicobacter pylori and ubiquitin-protein ligase E3 component n-recognin 2 were detected in most of the AIP patients tested, as well as a small number of PDAC cases [35]. It would be interesting to combine our proteomic model with testing for those autoantigens for diagnosis of chronic pancreatic diseases.

In this study, 2 acute pancreatitis patients and 14 healthy subjects were assigned to the cancerous group by our 7-signal proteomic model in the training (7 healthy subjects) and test (2 acute pancreatitis patients and 7 healthy subjects) cohorts. Since that time, we have carefully followed their clinical courses of these healthy subjects and found that 5 suffered from cancerous disease within 3 years, including 2 with rectal cancer, 1 with prostate cancer, 1 with hepatocellular carcinoma, and 1 with a metastatic bone tumor from an unknown primary site. In addition, another false positive healthy subject later developed polyposis in the colon. These observations suggest potential relation of our proteomic model with these malignancies, although further in-depth investigations are apparently required to draw definitive conclusions.

Mass spectrometry profiles obtained from complex protein mixtures can contain thousands of data points derived from real protein signatures. However, they can also be contaminated by electronic and chemical noise, variability in instrumentation, and variable crystallization of the matrix, necessitating careful analytical techniques [11, 13, 14]. In the present study, we employed multiple statistical methods and leave-one-out cross-validation to combine differentially expressed proteins with the clinical variables and found that a minimal set of 7 low-molecular weight proteins was sufficient to distinguish between healthy subjects and PDAC patients. The discriminating power of the extracted proteomic signature was further validated using independent test datasets obtained from plasma specimens collected at 2 different institutions. With this protocol, we carefully eliminated accidental identification of overly optimistic and nonbiological/mathematical multivariate signatures within a closed cohort by overfitting.

The primary goal of this study was development of a bioassay applicable to clinical practice for detection of PDAC and discrimination from AIP, as attempts to identify proteins that comprise a proteomic model have not been fully successful to date. However, the high reproducibility of MALDI MS indicates that direct application of its findings would be successful. In the previous study, Koomen et al. reported that a set of 4 peaks could be used to detect PDAC, of which one MS signal was downregulated in PDAC patients and found to be derived from apolipoprotein A-I [23], while Yan et al. found that transthyretin levels were independently associated with PDAC likelihood when obstructive jaundice was considered [36]. Accordingly, our identification of apolipoprotein A-I and transthyretin, which is a constituent of our proteomic model and downregulated in PDAC patients in this study, is in accord with previous reports from different institutes. We also identified the downregulation of apolipoprotein C-III in serum samples obtained from PDAC patients [37, 38]. Further investigations are warranted to identify discriminating proteins for ascertainment of their functional significance. Notably, 2 downregulated peaks (8765 and 13762 m/z), which were previously extracted as proteomic serum markers for lung cancer [39], were also identified as downregulated proteomic signals in PDAC patients in the present study.

Prospective multi-institutional studies with a larger number of patients including those with early-stage PDAC, AIP, and other pancreatic diseases are apparently warranted to validate further significance of our 7-signal proteomic signature for clinical application. Given that it has potential for early detection of PDAC as well as accurate discrimination of AIP, our 7-signal proteomic model may ultimately lead to a reduction in the large number of deaths caused by devastating cancer and also provide better management for chronic inflammatory disease of pancreas.

Ethical Approval

Requisite approval from the institutional review boards and written informed consent from all subjects were obtained.

Acknowledgments

This work was supported in part by a Grant-in-Aid for Exploratory Research and Program for Improvement of Research Environment for Young Researchers from Special Coordination Funds for Promoting Science and Technology commissioned and a Grant-in-Aid for Scientific Research on Priority Areas, a Grant-in-Aid for Scientific Research (C) by the Ministry of Education, Culture, Sports, Science and Technology of Japan. The sponsors of the study had no role in its design, data collection, analysis, and interpretation of data, the decision to submit the manuscript for publication, or writing the manuscript.

References

[1] http://ganjoho.ncc.go.jp/public/statistics/backnumber/2009_en.html
[2] http://www.cancer.gov/cancertopics/types/pancreatic.
[3] M. Yamamoto, O. Ohashi, and Y. Saitoh, "Japan pancreatic cancer registry: current status," *Pancreas*, vol. 16, no. 3, pp. 238–242, 1998.

[4] M. Goggins, M. Canto, and R. Hruban, "Can we screen high-risk individuals to detect early pancreatic carcinoma?" *World Journal of Surgical Oncology*, vol. 74, no. 4, pp. 243–248, 2000.

[5] R. A. Abrams, L. B. Grochow, A. Chakravarthy et al., "Intensified adjuvant therapy for pancreatic and periampullary adenocarcinoma: survival results and observations regarding patterns of failure, radiotherapy dose and CA 19-9 levels," *International Journal of Radiation Oncology Biology Physics*, vol. 44, no. 5, pp. 1039–1046, 1999.

[6] R. E. Ritts and H. A. Pitt, "CA 19-9 in pancreatic cancer," *Surgical Oncology Clinics of North America*, vol. 7, no. 1, pp. 93–101, 1998.

[7] H. Hamano, S. Kawa, A. Horiuchi et al., "High serum IgG4 concentrations in patients with sclerosing pancreatitis," *The New England Journal of Medicine*, vol. 344, no. 10, pp. 732–738, 2001.

[8] D. L. Finkelberg, D. Sahani, V. Deshpande, and W. R. Brugge, "Autoimmune pancreatitis," *The New England Journal of Medicine*, vol. 355, no. 25, pp. 2670–2676, 2006.

[9] T. Pickartz, J. Mayerle, and M. M. Lerch, "Autoimmune pancreatitis," *Nature Clinical Practice Gastroenterology & Hepatology*, vol. 4, no. 6, pp. 314–323, 2007.

[10] F. Taguchi, B. Solomon, V. Gregorc et al., "Mass spectrometry to classify non-small-cell lung cancer patients for clinical outcome after treatment with epidermal growth factor receptor tyrosine kinase inhibitors: a multicohort cross-institutional study," *Journal of the National Cancer Institute*, vol. 99, no. 11, pp. 838–846, 2007.

[11] E. F. Petricoin, A. M. Ardekani, B. A. Hitt et al., "Use of proteomic patterns in serum to identify ovarian cancer," *The Lancet*, vol. 359, no. 9306, pp. 572–577, 2002.

[12] B. L. Adam, Y. Qu, J. W. Davis et al., "Serum protein fingerprinting coupled with a pattern-matching algorithm distinguishes prostate cancer from benign prostate hyperplasia and healthy men," *Cancer Research*, vol. 62, no. 13, pp. 3609–3614, 2002.

[13] K. Yanagisawa, Y. Shyr, B. J. Xu et al., "Proteomic patterns of tumour subsets in non-small-cell lung cancer," *The Lancet*, vol. 362, no. 9382, pp. 433–439, 2003.

[14] K. Yanagisawa, S. Tomida, Y. Shimada, Y. Yatabe, T. Mitsudomi, and T. Takahashi, "A 25-signal proteomic signature and outcome for patients with resected non-small-cell lung cancer," *Journal of the National Cancer Institute*, vol. 99, no. 11, pp. 858–867, 2007.

[15] V. G. Tusher, R. Tibshirani, and G. Chu, "Significance analysis of microarrays applied to the ionizing radiation response," *Proceedings of the National Academy of Sciences of the United States of America*, vol. 98, no. 9, pp. 5116–5121, 2001.

[16] T. R. Golub, D. K. Slonim, P. Tamayo et al., "Molecular classification of cancer: class discovery and class prediction by gene expression monitoring," *Science*, vol. 286, no. 5439, pp. 531–527, 1999.

[17] R. Simon, M. D. Radmacher, K. Dobbin, and L. M. McShane, "Pitfalls in the use of DNA microarray data for diagnostic and prognostic classification," *Journal of the National Cancer Institute*, vol. 95, no. 1, pp. 14–18, 2003.

[18] M. B. Eisen, P. T. Spellman, P. O. Brown, and D. Botstein, "Cluster analysis and display of genome-wide expression patterns," *Proceedings of the National Academy of Sciences of the United States of America*, vol. 95, no. 25, pp. 14863–14868, 1998.

[19] A. Dupuy and R. M. Simon, "Critical review of published microarray studies for cancer outcome and guidelines on statistical analysis and reporting," *Journal of the National Cancer Institute*, vol. 99, no. 2, pp. 147–157, 2007.

[20] A. Ghazale, S. T. Chari, T. C. Smyrk et al., "Value of serum IgG4 in the diagnosis of autoimmune pancreatitis and in distinguishing it from pancreatic cancer," *American Journal of Gastroenterology*, vol. 102, no. 8, pp. 1646–1653, 2007.

[21] G. M. Fiedler, A. B. Leichtle, J. Kase et al., "Serum peptidome profiling revealed platelet factor 4 as a potential discriminating peptide associated with pancreatic cancer," *Clinical Cancer Research*, vol. 15, no. 11, pp. 3812–3819, 2009.

[22] K. Honda, Y. Hayashida, T. Umaki et al., "Possible detection of pancreatic cancer by plasma protein profiling," *Cancer Research*, vol. 65, no. 22, pp. 10613–10622, 2005.

[23] J. M. Koomen, L. N. Shih, K. R. Coombes et al., "Plasma protein profiling for diagnosis of pancreatic cancer reveals the presence of host response proteins," *Clinical Cancer Research*, vol. 11, no. 3, pp. 1110–1118, 2005.

[24] J. Koopmann, Z. Zhang, N. White et al., "Serum diagnosis of pancreatic adenocarcinoma using surface-enhanced laser desorption and ionization mass spectrometry," *Clinical Cancer Research*, vol. 10, no. 3, pp. 860–868, 2004.

[25] F. Safi, W. Schlosser, G. Kolb, and H. G. Beger, "Diagnostic value of CA 19-9 in patients with pancreatic cancer and non-specific gastrointestinal symptoms," *Journal of Gastrointestinal Surgery*, vol. 1, no. 2, pp. 106–112, 1997.

[26] H. Narimatsu, H. Iwasaki, F. Nakayama et al., "Lewis and secretor gene dosages affect CA19-9 and DU-PAN-2 serum levels in normal individuals and colorectal cancer patients," *Cancer Research*, vol. 58, no. 3, pp. 512–518, 1998.

[27] C. A. Iacobuzio-Donahue, A. Maitra, M. Olsen et al., "Exploration of global gene expression patterns in pancreatic adenocarcinoma using cDNA microarrays," *American Journal of Pathology*, vol. 162, no. 4, pp. 1151–1162, 2003.

[28] H. Han, D. J. Bearss, L. W. Browne, R. Calaluce, R. B. Nagle, and D. D. Von Hoff, "Identification of differentially expressed genes in pancreatic cancer cells using cDNA microarray," *Cancer Research*, vol. 62, no. 10, pp. 2890–2896, 2002.

[29] B. Ryu, J. Jones, N. J. Blades et al., "Relationships and differentially expressed genes among pancreatic cancers examined by large-scale serial analysis of gene expression," *Cancer Research*, vol. 62, no. 3, pp. 819–826, 2002.

[30] R. M. Caprioli, T. B. Farmer, and J. Gile, "Molecular imaging of biological samples: localization of peptides and proteins using MALDI-TOF MS," *Analytical Chemistry*, vol. 69, no. 23, pp. 4751–4760, 1997.

[31] S. A. Schwartz, R. J. Weil, R. C. Thompson et al., "Proteomic-based prognosis of brain tumor patients using direct-tissue matrix-assisted laser desorption ionization mass spectrometry," *Cancer Research*, vol. 65, no. 17, pp. 7674–7681, 2005.

[32] M. Stoeckli, P. Chaurand, D. E. Hallahan, and R. M. Caprioli, "Imaging mass spectrometry: a new technology for the analysis of protein expression in mammalian tissues," *Nature Medicine*, vol. 7, no. 4, pp. 493–496, 2001.

[33] M. Ehmann, K. Felix, D. Hartmann et al., "Identification of potential markers for the detection of pancreatic cancer through comparative serum protein expression profiling," *Pancreas*, vol. 34, no. 2, pp. 205–214, 2007.

[34] J. Guo, W. Wang, P. Liao et al., "Identification of serum biomarkers for pancreatic adenocarcinoma by proteomic analysis," *Cancer Science*, vol. 100, no. 12, pp. 2292–2301, 2009.

[35] L. Frulloni, C. Lunardi, R. Simone et al., "Identification of a novel antibody associated with autoimmune pancreatitis," *The New England Journal of Medicine*, vol. 361, no. 22, pp. 2135–2142, 2009.

[36] L. Yan, S. Tonack, R. Smith et al., "Confounding effect of obstructive jaundice in the interpretation of proteomic plasma profiling data for pancreatic cancer," *Journal of Proteome Research*, vol. 8, no. 1, pp. 142–148, 2009.

[37] H. L. Huang, T. Stasyk, S. Morandell et al., "Biomarker discovery in breast cancer serum using 2-D differential gel electrophoresis/MALDI-TOF/TOF and data validation by routine clinical assays," *Electrophoresis*, vol. 27, no. 8, pp. 1641–1650, 2006.

[38] R. D. Oleschuk, M. E. McComb, A. Chow et al., "Characterization of plasma proteins adsorbed onto biomaterials by MALDI- TOFMS," *Biomaterials*, vol. 21, no. 16, pp. 1701–1710, 2000.

[39] P. B. Yildiz, Y. Shyr, J. S. M. Rahman et al., "Diagnostic accuracy of MALDI mass spectrometric analysis of unfractionated serum in lung cancer," *Journal of Thoracic Oncology*, vol. 2, no. 10, pp. 893–901, 2007.

Bioorganic & Medicinal Chemistry Letters 22 (2012) 1731–1733

Contents lists available at SciVerse ScienceDirect

Bioorganic & Medicinal Chemistry Letters

journal homepage: www.elsevier.com/locate/bmcl

Hybrid liposomes affect cellular lipid constituents and caveolae structures

Ke Cao [a], Kouji Tanaka [b], Yuji Komizu [c], Keiko Tamiya-Koizumi [d], Takashi Murate [d], Ryuichi Ueoka [c], Mamoru Kyogashima [e], Jiro Usukura [f], Takashi Takahashi [a], Motoshi Suzuki [a,*]

[a] Division of Molecular Carcinogenesis, Nagoya University Graduate School of Medicine, Nagoya 466-8550, Japan
[b] Department of Oncology, Graduate School of Pharmaceutical Science, Nagoya City University, Nagoya 464-8681, Japan
[c] Division of Applied Life Science, Graduate School of Engineering, Sojo University, Kumamoto 860-0082, Japan
[d] Department of Medical Technology, Nagoya University Graduate School of Health Sciences, Nagoya 461-8673, Japan
[e] Department of Microbiology and Molecular Cell Biology, Nihon Pharmaceutical University, Saitama 362-0806, Japan
[f] Research Facility in Advanced Science and Technology, EcoTopia Science Institute, Nagoya University, Nagoya 464-8603, Japan

ARTICLE INFO

Article history:
Received 25 October 2011
Revised 5 December 2011
Accepted 20 December 2011
Available online 28 December 2011

Keywords:
Hybrid liposomes
Phosphatidylcholine
Cancer
Caveolae

ABSTRACT

We examined alterations of lipid constituents induced by hybrid liposomes (HLs) in cancer cells. As early as 1 h after HL treatment, amounts of the raft/caveolae lipids sphingomyelin, ceramide, and ether-type PC were altered. In addition, the structures of caveolae on the cytoplasmic surface of the cell membrane were significantly changed. Our results suggest that alterations of lipid composition in caveolae mediate HL signaling for apoptosis.

Hybrid liposomes† (HLs)[1] contain 90 mol % L-α-dimyristoylphosphatidylcholine (DMPC, NOF, Tokyo, Japan) and 10 mol % polyoxyethylene(n) dodecyl ether ($C_{12}(EO)_n$, $n = 23$, Sigma Chemicals, St Louis, MO) in a 5% glucose solution.[2] They have been shown effective for inhibiting the growth of various tumor cells in vitro,[3,4] in vivo in animal models,[5,6] and in a clinical patient.[7]

HLs are fused and accumulate in tumor cell membranes, and their apoptosis signals are passed through caspases-9, -3, and -8.[2] However, which signals initially activate these apoptotic pathways have yet to be elucidated. In that regard, we analyzed the lipid constituents in HL-treated SH-SY5Y and LS174T cells.

In accord with previous results, HLs reduced the viable cell population (Fig. 1). Under these conditions, the total amounts of the glycerophospholipids PC, PE, PI, and PS were not significantly different between the HL-treated and control cells (Supplementary Fig. 1).

Since DMPC is the major HL component, we further analyzed PC species. In the absence of HLs, we were unable to detect DMPC in SH-SY5Y and LS174T cells. In contrast, HL-treated cells were found to contain DMPC, and had decreased amounts of ether- and other types of diacyl-PC (Fig. 2A, B). Also, MALDI-TOF MS analysis revealed that in addition to DMPC, the levels of PC with C30:0 (hereinafter abbreviated as C30:0) in SH-SY5Y cells and C32:1 in LS174T were also increased (Fig. 2C, D). C30:0 and C32:1 may be metabolic products of DMPC, generated by re-acylation of excised and elongated myristic acid. In contrast, the cells were associated with a global decrease in PC species with longer acyl chains.

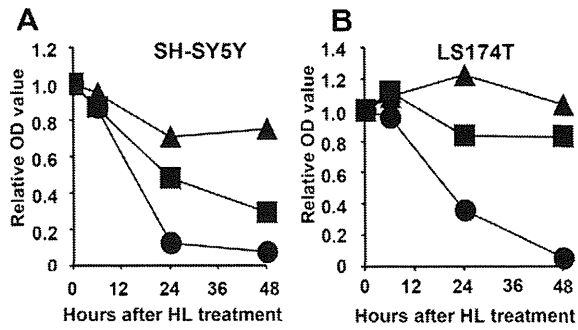

Figure 1. Apoptosis induction. SH-SY5Y (A) or LS-174T (B) cells were cultured in 500 μl of culture medium in 24-well plates at a density of 5×10^4 per well for 16 h. Medium was replaced with that containing various concentrations of HLs, followed by incubation for up to 48 h. Viable cells were determined in triplicate using TetraColor One (Seikagaku, Tokyo, Japan) with reference to the viability of mock-treated cells.[8] Triangle, square, and circle represent cells treated with 50, 100 and 200 μM, respectively, of HLs. Error bars are shown when errors exceed the symbols.

* Corresponding author. Tel.: +81 52 744 2456; fax: +81 52 744 2457.
E-mail address: msuzuki@med.nagoya-u.ac.jp (M. Suzuki).

† Abbreviations: HLs, hybrid liposomes; PC, phosphatidylcholine; DMPC, dimyristoylphosphatidylcholine; PC, PE, PI and PS are glycerophospholipid containing choline, ethanolamine, inositol and serine.

0960-894X/$ - see front matter © 2011 Elsevier Ltd. All rights reserved.
doi:10.1016/j.bmcl.2011.12.093

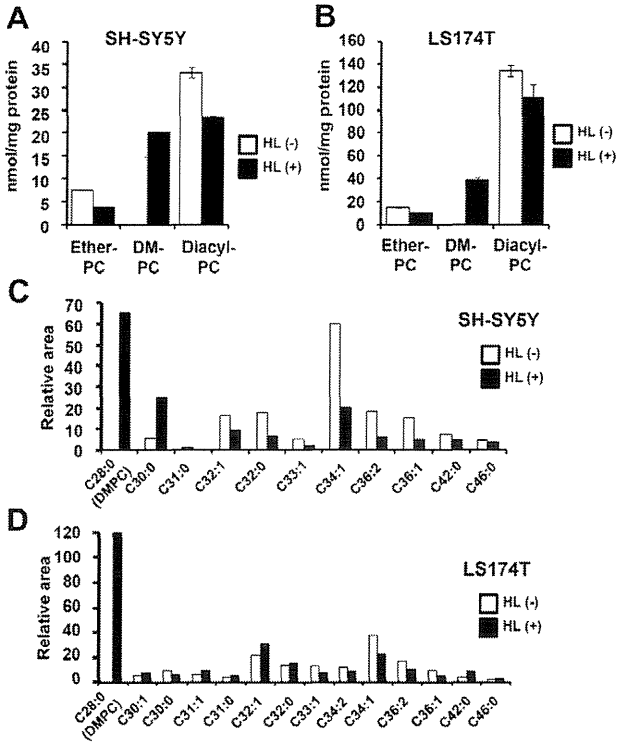

Figure 2. Molecular species of PC. (A, B) Total PC prepared by Folch's method[9] was subjected to mild alkaline hydrolysis.[10] An alkali-stable PC fraction containing an alkenyl- or alkyl-chain was designated as ether-PC. The amount of diacyl-PC was calculated by subtracting the amounts of ether- and DM-PC from total PC. (C, D). PC species were analyzed in positive ion mode using an AXIMA Performance mass spectrometer (Shimadzu/Kratos, UK) equipped with a nitrogen UV laser (337 nm). Sphingosylphosphorylcholine was mixed with the PC extracts, and used as the standard. Areas corresponding to each PC were calculated and are shown as graphs. DMPC was designated as C28:0. HL (+) and HL (−) represent results obtained with and without HLs, respectively.

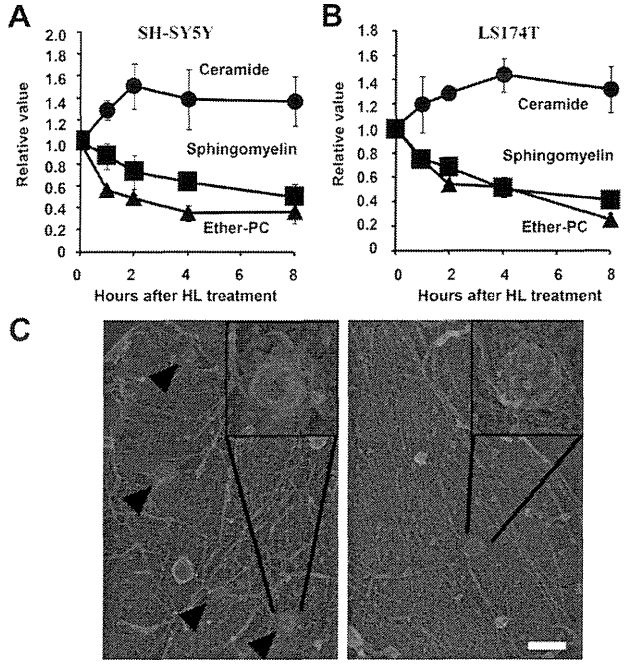

Figure 3. Alterations in caveolae constituents and structures. (A, B) Ceramide was separated from total lipids by thin-layer chromatography (TLC) and developed using $CHCl_3$/MeOH/acetic acid (94:1:5, v/v). Sphingomyelin and ether-PC (Fig. 2) were separated from alkali-stable lipid fractions by TLC, and developed using $CHCl_3$/MeOH/H_2O (65:25:4, v/v). Each lipid band was visualized after spraying 0.1% primulin in acetone/H_2O (Sigma, >4:1,v/v) and UV irradiation, and quantified using ImageJ (NIH, Bethesda, MD). Intensity at 0 h was designated as 1. (C) SH-SY5Y cells were cultured with 200 μM HL for 0 (left) or 1 (right) hour, then their submembrane structures were subjected to ultramicroscopic analysis. Arrowheads indicate caveolae. Some are enlarged and shown in inlets. White bar indicates 1 μm.

Among the sphingolipids, HL treatment resulted in a decrease in sphingomyelin and an increase in ceramide (Fig. 3A, B), as early as 1 h after HL addition. HL addition might have induced hydrolysis of sphingomyelin by neutral sphingomyelinases in the plasma membrane, resulting in ceramide production. It is also likely that DMPC competitively inhibited sphingomyelin synthases, which catalyse phosphocholine transfer from PC to ceramide. This inhibition may lead to ceramide increase and sphingomyelin decrease. It was also found that ether-PC was decreased in a similar manner as sphingomyelin (Fig. 3A, B).

Since sphingolipids and ether-PC are the major components of the detergent-resistant membrane micro-domain raft/caveolae,[11–13] alterations of these lipids may affect the structures and functions of members of this micro-domain. To investigate these phenomena, we visualized the membrane undercoat of the vertical cell surface using a freeze-etching replica method.[14] One hour after HL treatment, we found a change in the membrane skeleton. In control cells, actin filaments extended over the membrane surface, whereas they were firmly attached to the surface in the HL-treated cells. Furthermore, we were unable to find typical caveolae structures in HL-treated cells, except for distorted structures (Fig. 3C).

In summary, HL treatment altered the amounts of ether-PC, sphingomyelin, and ceramide, which may have also resulted in alterations of the caveolae structures. Since caveolae play essential roles in signal transduction, the HL-treated cells likely generated ill-signals and fallen into apoptosis. It has been proposed that ceramide plays an important role in the apoptotic signaling pathway.[15,16] Therefore, we do not rule out the possibility that a certain type of ceramide played a role as a second messenger, leading to apoptosis. In this manuscript, we have focused on the alterations in the phospho- and sphingolipids compositions. With the concentration employed in our experiments, contribution extent of $C_{12}(EO)_{23}$, the second component of HL, to apoptosis signaling may be limited, because $C_{12}(EO)_{23}$ has been primarily considered to function for vesicle -fluidity and -uptake into cells.[17–20] Further analysis and identification of HL-induced apoptosis pathways may provide the basis for future cancer treatment.

Acknowledgments

This work was supported in part by a Grant-in-Aid for Scientific Research on Innovative Areas from the Ministry of Education, Culture, Sports, Science, and Technology of Japan, and a Grant-in-Aid for Scientific Research from the Japan Society for the Promotion of Science. We thank Dr. Mitsuhiro Nakamura of Gifu Pharmaceutical University and Dr. Yoshiko Banno for Gifu University Graduate School of Medicine for the critical discussion.

Supplementary data

Supplementary data associated with this article can be found, in the online version, at doi:10.1016/j.bmcl.2011.12.093.

References and notes

1. Ueoka, R.; Matsumoto, Y.; Robert, A.; Swarup, S.; Sugii, A.; Harada, K.; Kikuchi, J.; Murakami, Y. *J. Am. Chem. Soc.* **1988**, *110*, 1588.
2. Matsumoto, Y.; Iwamoto, Y.; Matsushita, T.; Ueoka, R. *Int. J. Cancer* **2005**, *115*, 377.
3. Komizu, Y.; Nakata, S.; Goto, K.; Matsumoto, Y.; Ueoka, R. A. C. S. *Med. Chem. Lett.* **2011**, *2*, 275.

4. Towata, T.; Komizu, Y.; Kariya, R.; Suzu, S.; Matsumoto, Y.; Kobayashi, N.; Wongkham, C.; Wongkham, S.; Ueoka, R.; Okada, S. *Bioorg. Med. Chem. Lett.* **2010**, *20*, 3680.
5. Ichihara, H.; Ueno, J.; Umebayashi, M.; Matsumoto, Y.; Ueoka, R. *Int. J. Pharm.* **2011**, *406*, 173.
6. Towata, T.; Komizu, Y.; Suzu, S.; Matsumoto, Y.; Ueoka, R.; Okada, S. *Leuk. Res.* **2010**, *34*, 906.
7. Ichihara, H.; Nagami, H.; Kiyokawa, T.; Matsumoto, Y.; Ueoka, R. *Anticancer Res.* **2008**, *28*, 1187.
8. Huang, Q. M.; Tomida, S.; Masuda, Y.; Arima, C.; Cao, K.; Kasahara, T. A.; Osada, H.; Yatabe, Y.; Akashi, T.; Kamiya, K.; Takahashi, T.; Suzuki, M. *Cancer Res.* **2010**, *70*, 8407.
9. Folch, J.; Lees, M.; Sloane Stanley, G. H. *J. Biol. Chem.* **1957**, *226*, 497.
10. Dawson, R. M. *Biochem. J.* **1960**, *75*, 45.
11. Kiyokawa, E.; Baba, T.; Otsuka, N.; Makino, A.; Ohno, S.; Kobayashi, T. *J. Biol. Chem.* **2005**, *280*, 24072.
12. Matsumori, N.; Okazaki, H.; Nomura, K.; Murata, M. *Chem. Phys. Lipids* **2011**, *164*, 401.
13. Milhas, D.; Clarke, C. J.; Hannun, Y. A. *FEBS Lett.* **2010**, *584*, 1887.
14. Morone, N.; Fujiwara, T.; Murase, K.; Kasai, R. S.; Ike, H.; Yuasa, S.; Usukura, J.; Kusumi, A. *J. Cell Biol.* **2006**, *174*, 851.
15. Hannun, Y. A. *Science* **1996**, *274*, 1855.
16. Stiban, J.; Tidhar, R.; Futerman, A. H. *Adv. Exp. Med. Biol.* **2010**, *688*, 60.
17. Kao, K. N.; Constabel, F.; Michayluk, M. R.; Gamborg, O. L. *PLANTA* **1974**, *115*, 355.
18. Nagami, H.; Matsumoto, Y.; Ueoka, R. *Int. J. Pharm.* **2006**, *315*, 167.
19. Komizu, Y.; Ueoka, H.; Goto, K.; Ueoka, R. *Int. J. Nanomedicine* **2011**, *6*, 1913.
20. Komizu, Y.; Yukihara, M.; Kariya, R.; Goto, K.; Okada, S.; Ueoka, R. *Bioorg. Med. Chem. Lett.* **2011**, *21*, 3962.

Published OnlineFirst February 16, 2012; DOI:10.1158/0008-5472.CAN-11-3878

Molecular and Cellular Pathobiology

Cancer Research

Tumor Cell–Derived Angiopoietin-like Protein ANGPTL2 Is a Critical Driver of Metastasis

Motoyoshi Endo[1], Masahiro Nakano[1,2], Tsuyoshi Kadomatsu[1], Shigetomo Fukuhara[3], Hiroaki Kuroda[4], Shuji Mikami[5], Tai Hato[4,6], Jun Aoi[1], Haruki Horiguchi[1], Keishi Miyata[1], Haruki Odagiri[1], Tetsuro Masuda[1], Masahiko Harada[6], Hirotoshi Horio[6], Tsunekazu Hishima[7], Hiroaki Nomori[4], Takaaki Ito[8], Yutaka Yamamoto[2], Takashi Minami[9], Seiji Okada[10], Takashi Takahashi[11], Naoki Mochizuki[3], Hirotaka Iwase[2], and Yuichi Oike[1]

Abstract

Strategies to inhibit metastasis have been mainly unsuccessful in part due to insufficient mechanistic understanding. Here, we report evidence of critical role for the angiopoietin-like protein 2 (ANGPTL2) in metastatic progression. In mice, *Angptl2* has been implicated in inflammatory carcinogenesis but it has not been studied in human tumors. In patients with lung cancer, elevated levels of ANGPTL2 expression in tumor cells within the primary tumor were associated with a reduction in the period of disease-free survival after surgical resection. Transcription factors NFATc, ATF2, and c-Jun upregulated in aggressive tumor cells promoted increased *Angptl2* expression. Most notably, tumor cell–derived ANGPTL2 increased *in vitro* motility and invasion in an autocrine/paracrine manner, conferring an aggressive metastatic tumor phenotype. In xenograft mouse models, tumor cell–derived ANGPTL2 accelerated metastasis and shortened survival whereas attenuating ANGPTL2 expression in tumor cells–blunted metastasis and extended survival. Overall, our findings showed that tumor cell–derived ANGPTL2 drives metastasis and provided an initial proof of concept for blockade of its action as a strategy to antagonize the metastatic process. *Cancer Res; 72(7); 1784–94. ©2012 AACR.*

Introduction

Cancer is a leading cause of death and accounts for 7.6 million deaths (~13% of all deaths) worldwide (1). Although both diagnosis and therapeutic modalities used to treat cancer have remarkably improved, tumor metastasis still represents a major cause of cancer mortality (2, 3). Therefore, identification of mechanisms underlying metastasis is essential to understand the pathophysiology of this lethal condition and identify novel therapeutic targets.

Authors' Affiliations: Departments of [1]Molecular Genetics, [2]Breast and Endocrine Surgery, Kumamoto University, Kumamoto; [3]Department of Structural Analysis, National Cardiovascular Center Research Institute, Osaka; Departments of [4]General Thoracic Surgery and [5]Diagnostic Pathology, Keio University; Departments of [6]General Thoracic Surgery and [7]Pathology, Tokyo Metropolitan Cancer and Infectious Diseases Center Komagome Hospital; [8]Departments of Pathology and Experimental Medicine, Kumamoto University, Kumamoto; [9]Research Center for Advanced Science and Technology, University of Tokyo, Tokyo; and [10]Center for AIDS Research Center, Kumamoto University, Kumamoto; and [11]Division of Molecular Carcinogenesis, Center for Neurological Diseases and Cancer, Nagoya University Graduate School of Medicine, Nagoya, Japan

Note: Supplementary data for this article are available at Cancer Research Online (http://cancerres.aacrjournals.org/).

M. Endo, M. Nakano, and T. Kadomatsu contributed equally to this work.

Corresponding Author: Yuichi Oike, Department of Molecular Genetics, Kumamoto University, 1-1-1 Honjo, Kumamoto 860-8556, Japan. Phone: 81-96-373-5140; Fax: 81-96-373-5145; E-mail: oike@gpo.kumamoto-u.ac.jp

doi: 10.1158/0008-5472.CAN-11-3878

Inflammation plays key roles at various stages of tumor development, including initiation, growth, invasion, and metastasis (4). Recently, we found that angiopoietin-like protein 2 (ANGPTL2) increases inflammatory carcinogenesis in a chemically induced skin squamous cell carcinoma (SCC) mouse model through enhanced susceptibility to "preneoplastic change" and "malignant conversion" (5). In addition, we also reported that ANGPTL2 expression in tumor cells is highly correlated with the frequency of tumor cell metastasis to distant organs and lymph nodes through increased tumor angiogenesis and tumor cell epithelial-to-mesenchymal transitions (EMT; ref. 5). However, it has been obscure whether ANGPTL2 contributes to human cancer pathogenesis.

The nuclear factor of activated T cell (NFATc) consists of 5 members (NFATc1–c4 and NFAT5). Among these factors, NFATc1–c4 function in tumor cell development and metastasis (6, 7). For example, NFATc1 and NFATc3 contribute to the pathogenesis of melanoma and pancreatic cancer (8, 9), NFATc2 plays role in breast cancer cell migration and invasion (10), and NFATc4 promotes breast cancer cell growth (11).

In the present study, we investigated the role of ANGPTL2 in human tumor cells and found that patients with lung cancer showing high ANGPTL2 expression in cells within the primary tumor sites showed poor prognosis in terms of disease-free survival. Furthermore, we found that *Angptl2* expression in tumor cells is induced by NFATc. Tumor cell–derived ANGPTL2 enhanced tumor cell motility and invasive capacity and increased tumor angiogenesis. Tumor cell–derived ANGPTL2 also accelerated metastasis and shortened survival periods in tumor cell–implanted mouse models. In contrast,

Published OnlineFirst February 16, 2012; DOI:10.1158/0008-5472.CAN-11-3878

decreasing ANGPTL2 levels in tumor cells attenuated metastasis and prolonged survival periods. Collectively, our findings provide strong evidence that tumor cell–derived ANGPTL2 worsens clinical prognosis and suggest that blocking ANGPTL2 could represent a novel therapeutic strategy to inhibit tumor metastasis.

Materials and Methods

Quantitation of ANGPTL2 protein by ELISA

ANGPTL2 concentrations in tissue lysates or in culture medium from tumor cells were estimated by an ANGPTL2 Assay Kit (IBL), as described (12, 13). For tissue lysates, proteins were extracted from 2 mg of tumor or nontumor tissue and dissolved in 10 mL lysis buffer [300 mmol/L NaCl, 50 mmol/L Tris-HCl (pH 7.5), 1% Triton X-100, and 1mmol/L EDTA].

Immunohistochemistry and *in situ* hybridization

Immunohistochemical and *in situ* hybridization analyses were conducted as described (12, 14). Antibodies for CD44 (Abcam), paxillin (BD Bioscience), and rhodamine-phalloidin (Molecular Probes) were purchased. We also used an anti-ANGPTL2 antibody that we generated (12, 14).

Cell lines and cell culture

The human lung cancer cell lines NCI-H460 and NCI-H460-LNM35 cells, as previously described (15), were provided by T. Takahashi (Nagoya University, Nagoya, Japan). H460 and LNM35 cells were cultured in RPMI-1640 medium supplemented with 10% fetal calf serum. The human breast adenocarcinoma cell lines T47D, MDA-MB453, and MDA-MB231 were purchased from the American Type Culture Collection that carries out cell line characterizations and passaged in our laboratory for fewer than 6 months after receipt. Detailed information about establishment of stable cell lines is provided in the Supplementary Methods.

Luciferase assay

H460 cells were incubated for 48 hours after cotransfection with indicated expression and reporter plasmids and phRL-TK vector (Promega). Luciferase activities were determined by a Dual-Luciferase Reporter Assay System (Promega). For some experiments, transfected cells were incubated with 10 ng/mL phorbol 12-myristate 13-acetate (PMA) or with 10 ng/mL PMA plus 1 μmol/L ionomycin (PMA/Ion) for 24 hours. Details relevant to expression and reporter plasmids are provided in the Supplementary Methods.

Real-time quantitative reverse transcriptase PCR

Real-time quantitative reverse transcriptase PCR was carried out as described (12). Oligonucleotide primers are listed in Supplementary Table S1.

Immunoblot analysis

Immunoblot analysis was conducted as described (5). Antibodies used were against NFATc2 (BD Bioscience), ATF2 (N-96; Santa Cruz), c-Jun (D; Santa Cruz), and ANGPTL2 (13).

Cell invasion assay

Cell invasiveness was estimated by a 96-well BME Cell Invasion Assay Kit (Trevigen) according to the manufacturer's protocol. Fluorescence was measured with a Fluoroskan Ascent fluorometer (Thermo Labsystems).

Time-lapse microscopy and FRET imaging

Cell migration was monitored by time-lapse microscopy with an Olympus IX-81 inverted microscope with a 20× objective lens. Phase contrast images were collected with CoolSNAP-HQ (Roper Scientific) at 3-minute intervals. A series of time-lapse images was converted to video format with MetaMorph 6.1 software. Cell motility was quantified with MetaMorph 6.1 software. Fluorescence resonance energy transfer (FRET) imaging was carried out as described (13).

Human studies

All studies were approved by the Ethics Committee of Kumamoto University, Keio University (Tokyo, Japan), or the Tokyo Metropolitan Cancer and Infectious Diseases Center of Komagome Hospital. Written informed consent was obtained from each subject. Patient information is provided in Supplementary Methods.

Animal studies

All experiments were carried out according to guidelines of Institutional Animal Committee of Kumamoto University. Details relevant to the mouse model are provided in Supplementary Methods.

Statistics

The Kaplan–Meier log-rank test was used to analyze survival data of mice and patients with JMP7 software (SAS Institute). Data presented as means ± SD or means ± SEM were analyzed using the Student t test or ANOVA. A P value of less than 0.05 was considered significant.

Results

ANGPTL2 levels within primary tumor sites correlate with poor disease-free survival

To examine whether ANGPTL2 is expressed in human tumor tissues, we compared ANGPTL2 protein levels in lung tissues extracted from primary tumor sites in patients with non–small cell lung carcinoma (NSCLC) to those from peripheral nontumor lung tissue by an ELISA. ANGPTL2 protein levels in primary tumor sites were significantly greater than those seen in nontumor lung tissue (Fig. 1A). Given the variation in ANGPTL2 expression in tumor tissue (Fig. 1A), we examined ANGPTL2 expression in lung tumor tissues by immunohistochemistry. Accordingly, we observed wide variation in the proportion of cells within a tumor that express ANGPTL2 (Fig. 1B, Supplementary Fig. S1). *In situ* hybridization analysis (12) confirmed that tumor cells express *Angptl2* mRNA (Fig. 1C), indicating that tumor cells are the likely source of ANGPTL2 protein. In contrast to the variation in the proportion of ANGPTL2-expressing tumor cells within the primary tumor site, we observed high and homogeneous

Published OnlineFirst February 16, 2012; DOI:10.1158/0008-5472.CAN-11-3878

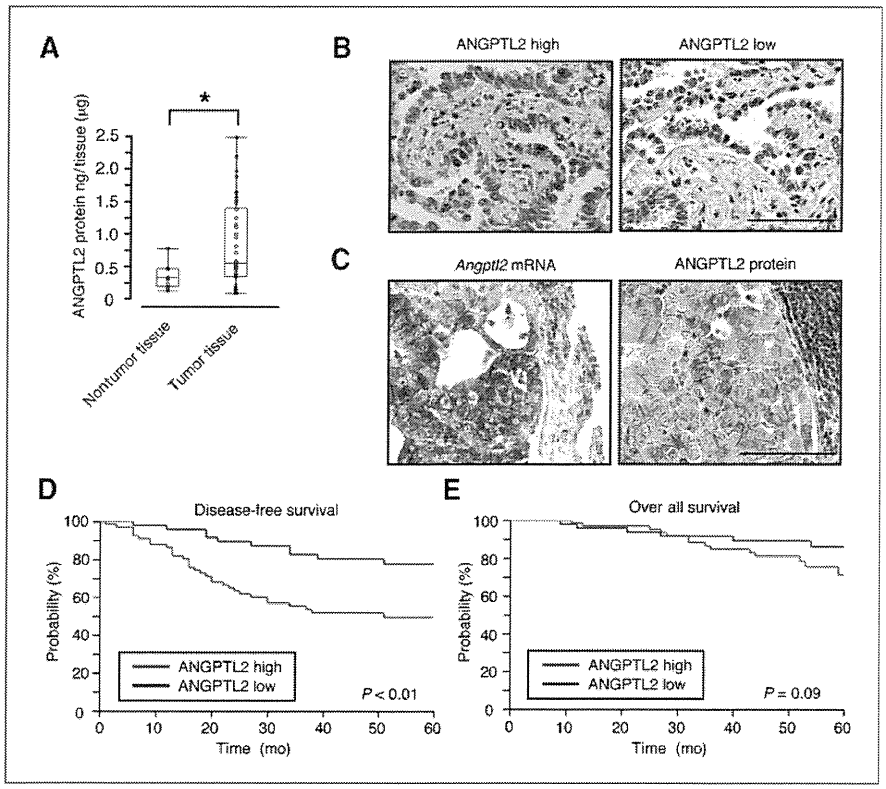

Figure 1. ANGPTL2 expression in tumor cells correlates with poor lung cancer prognosis. A, ANGPTL2 protein levels in lung tumor tissues ($n = 38$) and corresponding peripheral nontumor tissues ($n = 9$). B, ANGPTL2 immunostaining within the primary tumor. Groups from patients with NSCLC were defined as ANGPTL2 high and low, respectively. Scale bars, 100 μm. C, representative images of *Angptl2* mRNA and protein in serial tumor tissue sections from primary NSCLC. Scale bars, 100 μm. D–E, cohort of probability of disease-free survival (D) and overall survival (E) with ANGPTL2 high ($n = 66$) and low ($n = 48$) groups ($P < 0.01$ and $P = 0.09$ by log-rank test). *, $P < 0.05$.

expression of ANGPTL2 in tumor cells within metastasized tumor sites, including 3 brain tissues and 5 lymph nodes taken from 8 patients with lung cancer at autopsy (Supplementary Fig. S2), suggesting that ANGPTL2-positive tumor cells exhibit high metastatic capacity. We next divided patients with NSCLC into 2 groups based on the percentage of ANGPTL2-positive tumor cells within the primary tumor site: the high group was defined as showing greater than 20% of ANGPTL2-positive tumor cells and the low group showed fewer than 20%. Patients in the high group showed a shortened period of disease-free survival after surgery compared with the low group based on 2 independent cohort studies (Fig. 1D and E, Supplementary Fig. S3).

NFATc induces *Angptl2* expression in lung cancer cells

To investigate tumor cell regulation of *Angptl2* expression, we constructed luciferase reporter plasmids containing an *Angptl2* regulatory region that we identified from the human NSCLC cell line NCI-H460 (H460; Supplementary Fig. S4A). An F4 construct containing nucleotides −168 to +98 relative to the transcription start site of human *Angptl2* showed high reporter activity in H460 cells, whereas activity of an F5 construct (containing −21 to +98) showed significantly decreased activity, indicating that F4 contains elements regulate *Angptl2* expression in this context (Supplementary Fig. S4A). In that region, we identified potential binding sites for activating transcription factor/cAMP-responsive element–binding protein (ATF/CREB), NF-κB, and NFAT (Fig. 2A, top). To investigate whether these factors affect *Angptl2* expression, we transfected H460 cells with the F4 construct plus expression vectors encoding CREB, ATF2, ATF3, NF-κB, or a constitutively active form of NFATc (CA-NFATc). The CA-NFATc vector increased *Angptl2* reporter activity relative to a pcDNA3.1 control plasmid, whereas the other factors had no effect (Fig. 2A). Treatment of cells with a combination of PMA and ionomycin (PMA/Ion) stimulates calcium/calcineurin-dependent NFATc activation and induces its nuclear translocation (6, 16, 17). PMA/Ion treatment of H460 cells significantly increased *Angptl2* mRNA expression compared with controls, whereas treatment with the calcineurin inhibitor cyclosporin A (CsA) significantly blocked the PMA/Ion effect (Fig. 2B). These results suggest that NFATc functions in *Angptl2* expression in lung cancer cells.

ATF2 and c-Jun enhance NFATc-dependent *Angptl2* expression in lung cancer cells

It has been reported that activator protein (AP-1) components, c-Jun or c-Fos, form a stable heterodimer with ATF2, ATF3, or ATF4 and bind to the ATF/CREB site (18, 19). NFATc and AP-1 heterodimers form a transcriptional complex that synergistically activates target genes (20–22). We found that reporter activity of F4 constructs containing a mutant ATF/CREB site was markedly decreased relative to wild-type F4 constructs (Supplementary Fig. S4B), suggesting that ATF/CREB site is required for *Angptl2* expression. We observed that CA-NFATc–dependent induction of *Angptl2* reporter activity

Published OnlineFirst February 16, 2012; DOI:10.1158/0008-5472.CAN-11-3878

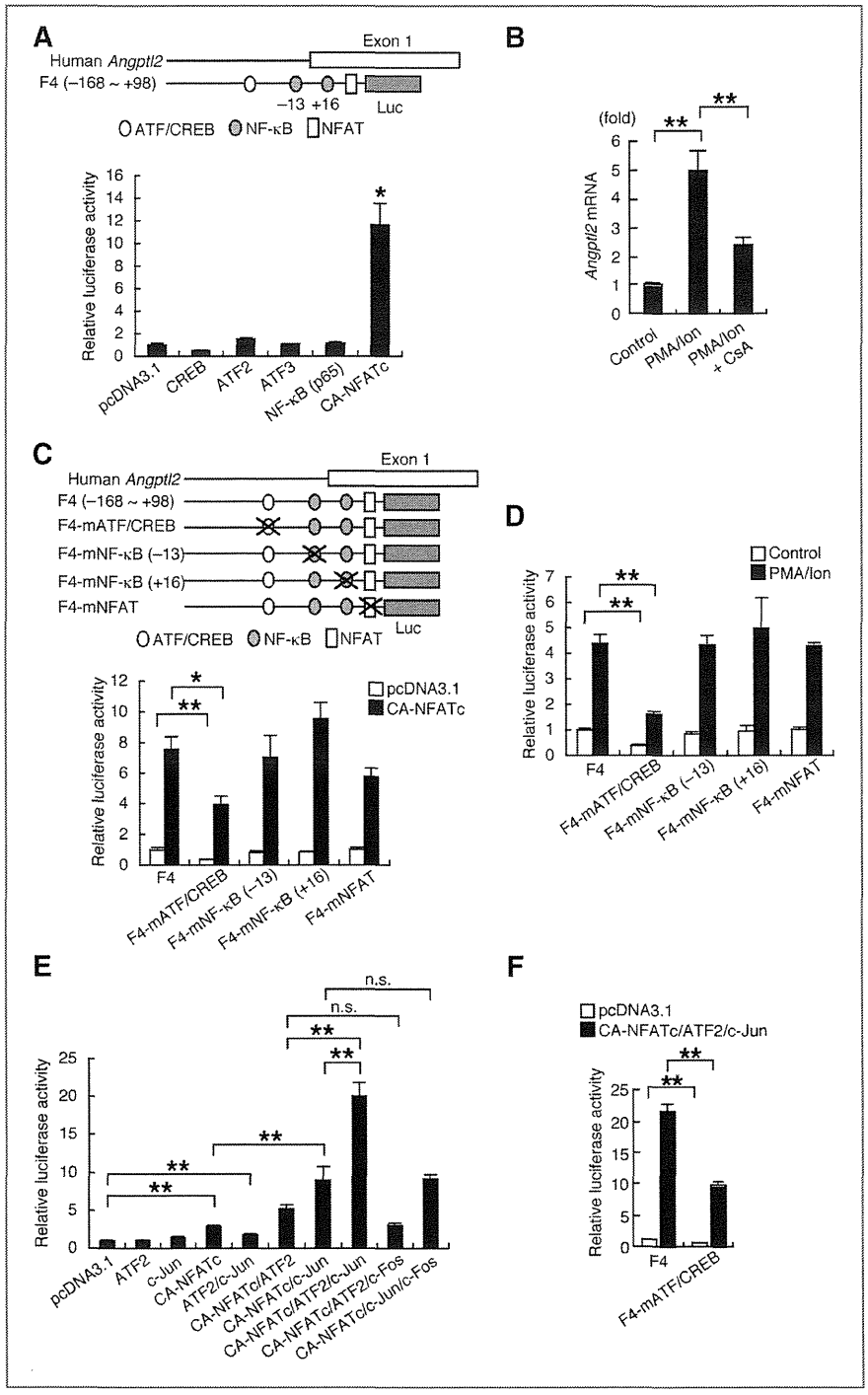

Figure 2. NFATc, ATF2, and c-Jun induce *Angptl2* expression. A, top, schematic diagram of the F4 construct and locations of putative transcription factor–binding sites. The white circle, gray circles, and white box indicate putative ATF/CREB site, NF-κB sites, and NFAT sites, respectively. Luc, luciferase. Bottom, comparison of relative luciferase activity among H460 cells cotransfected with the F4 construct plus CREB, ATF2, ATF3, NF-κB (p65), or CA-NFATc expression plasmids. Reporter activity of cells cotransfected with pcDNA3.1 was set at 1. B, relative *Angptl2* mRNA levels in H460 cells treated with PMA and ionomycin (PMA/Ion) with or without cyclosporin A (CsA). Levels in untreated cells (controls) were set at 1. C, top, schematic diagram of wild-type and mutant F4 constructs. Bottom, comparison of relative luciferase activity among H460 cells cotransfected with wild-type or mutant F4 constructs plus pcDNA3.1 or CA-NFATc expression plasmids. Reporter activity of cells cotransfected with wild-type F4 and pcDNA3.1 was set at 1. D, comparison of relative luciferase activity among H460 cells transfected with wild-type or mutant F4 constructs and treated with PMA/Ion. Reporter activity of cells transfected with the wild-type F4 construct but not treated with PMA/Ion was set at 1. E, comparison of relative luciferase activity among H460 cells cotransfected with F4 plus ATF2, c-Jun, CA-NFAT, or c-Fos expression plasmids or with a combination thereof. Reporter activity of cells cotransfected with pcDNA3.1 was set at 1. F, comparison of relative luciferase activity among H460 cells cotransfected with wild-type or mutant F4 constructs plus indicated expression plasmids (pcDNA3.1 or a CA-NFAT/ATF-2/c-Jun combination). Reporter activity of cells cotransfected with wild-type F4 plus pcDNA3.1 was set at 1. All experiments were carried out at least 3 times. Error bars show SEM. *, $P < 0.05$; **, $P < 0.01$; n.s., no statistical difference.

was also significantly suppressed in F4 constructs bearing a mutant compared with a wild-type ATF/CREB site (Fig. 2C). Furthermore, PMA/Ion treatment increased F4 reporter activity, an effect significantly decreased when we used F4 constructs harboring a mutant ATF/CREB site (Fig. 2D). Overall, it could be possible that NFATc forms a complex with AP-1 heterodimers that enhances NFATc-dependent induction of *Angptl2* expression through the ATF/CREB site. To investigate whether ATF family proteins may bind to ATF/CREB site on the *Angptl2* promoter region, we conducted an electrophoretic